Discovery of first-in-class imidazothiazole-based potent and selective ErbB4 (HER4) kinase inhibitors

Seyed-Omar Zaraei [a, b], Rawan M. Sbenati [c], Nour N. Alach [c], Hanan S. Anbar [d, **], Randa El-Gamal [e], Hamadeh Tarazi [c, f], Mahmoud K. Shehata [c], Mohammed S. Abdel-Maksoud [g], Chang-Hyun Oh [a, b], Mohammed I. El-Gamal [c, f, h, *]

[a] Center for Biomaterials, Korea Institute of Science and Technology, PO Box 131, Cheongryang, Seoul, 130-650, Republic of Korea
[b] Department of Biomolecular Science, Korea University of Science and Technology, 113 Gwahangno, Yuseong-gu, Daejeon, 305-333, Republic of Korea
[c] Sharjah Institute for Medical Research, University of Sharjah, Sharjah, 27272, United Arab Emirates
[d] Department of Clinical Pharmacy and Pharmacotherapeutics, Dubai Pharmacy College for Girls, Dubai, 19099, United Arab Emirates
[e] Department of Medical Biochemistry, Faculty of Medicine, University of Mansoura, Mansoura, 35516, Egypt
[f] Department of Medicinal Chemistry, College of Pharmacy, University of Sharjah, Sharjah, 27272, United Arab Emirates
[g] Medicinal & Pharmaceutical Chemistry Department, Pharmaceutical and Drug Industries Research Division, National Research Centre NRC (ID: 60014618)), Dokki, Giza, 12622, Egypt
[h] Department of Medicinal Chemistry, Faculty of Pharmacy, University of Mansoura, Mansoura, 35516, Egypt

ARTICLE INFO

ABSTRACT

This article reports on novel imidazothiazole derivatives as first-in-class potent and selective ErbB4 (HER4) inhibitors. There are no other reported selective inhibitors of this kinase in the literature, that's why they are considered as first-in-class. In addition, none of the reported non-selective ErbB4 inhibitors possesses imidazothiazole nucleus in its structure. Therefore, there is novelty in this work in both kinase selectivity and chemical structure. Compounds **Ik** and **IIa** are the most potent ErbB4 kinase inhibitor ($IC_{50} = 15.24$ and 17.70 nM, respectively). Compound **Ik** showed promising antiproliferative activity. It is selective towards cancer cell lines than normal cells. Its ability to penetrate T-47D cell membrane and inhibit ErbB4 kinase inside the cells has been confirmed. Moreover, both compound **Ik** and **IIa** have additional merits such as weak potency against hERG ion channels and against CYP 3A4 and 2D6. Molecular docking and dynamic simulation studies were carried out to explain binding interactions.

© 2021 Elsevier Masson SAS. All rights reserved.

1. Introduction

Cancer is one of the leading causes of death worldwide. Statistics show that by 2040, numbers of cancer incidence will continue to increase up to 29.5 million cases per year. Morbidity will rise to about 16.4 million cases around the world [1]. Because of these concerning statistics, extensive research is being done to find a therapeutically valuable agent for this disease.

One of the causes of cancer is dysregulated function of kinases that normally act as the on/off switch of cellular proliferation and motility [2]. Mutated kinases are responsible for cellular

abnormalities that can lead to cancer initiation, progression or metastasis. A number of kinase inhibitors has been approved by the FDA in the past years starting with imatinib as the first agent that gave evidence of the antiproliferative activity by means of kinase inhibition. Other kinase inhibitors have been approved later [3].

Among others, epidermal growth factor receptor (EGFR) plays a pivotal role in carcinogenesis. EGFR is a family of kinases of four subtypes, HER1, HER2, HER3, and HER4 [4,5]. While the first three kinases are studied thoroughly, HER4 (ErbB4) is yet to be under spotlight, despite the fact that evidence of correlation to initiation and progression of breast cancer has been established [6]. Studies have shown an involvement of ErbB4 with other cancers such as prostate cancer, colorectal cancer, ovarian cancer, lung cancer, gastric cancer, hepatocellular carcinoma, melanoma, bladder cancer, pancreatic cancer, and brain tumor [7–10]. The role of ErbB4 as anti- or pro-oncogenic is controversial. Some studies suggest that ErbB4 may inhibit tumor progression and proliferation, with

multiple studies arguing a better prognosis and survival for mammary tumor cells expressing ErbB4. While contradictory reports demonstrates a pro-oncogenic role of ErbB4 on tumor proliferation. RAS-MAPK-ERK and PI3K-Akt pathways are main downstream pathways linked to ErbB4, phosphorylation of ErbB4 leads to constant activation of RAS-MAPK-ERK and PI3K-Akt pathways leading to cell differentiation. The discrepancy of ErbB4 role in cancer can be rationalized by the presence of different ErbB4 splice variants, different dimers and natural ligands, multiple sites of phosphorylation, and various downstream signaling pathways. The lack of studies and reports of ErbB4's role in different cancers and the deficit of comprehensive understanding of its molecular signaling role can be traced to the lack of ErbB4 specific and selective ligands [10].

Different molecules have shown inhibitory activity of ErbB4 as shown in (Fig. 1). They can be classified chemically into quinazoline derivatives (allitinib, poziotinib, dacomitinib, lapatinib, afatinib, and canertinib), quinoline derivatives (neratinib and pyrotinib), pyrazolopyrimidine derivative (ibrutinib), and pyrrolotriazine derivative (AC-480). These molecules showed good potency against ErbB4 but suffer from lack of selectivity as they act as pan-HER inhibitors [11–20]. All of these compounds are irreversible kinase inhibitors except lapatinib and AC-480. In this study, a series of imidazo[2,1-b]thiazole compounds were synthesized, characterized and tested for their antiproliferative activity as kinase inhibitors. Based on our previous experience with kinase-inhibitory imidazothiazole derivatives [21–27], we designed and synthesized this series of compounds aiming at obtaining anticancer molecules with kinase-inhibiting activity. We investigated the impact of pyrimidine ring on activity through replacing it with phenyl. We also synthesized molecules possessing or lacking mesyl group to investigate its contribution to the activity. The phenyl ring was substituted with variety of substituents ranging from polar (e.g. hydroxyl, dimethylamino, diisopropylamino, pyrrolidine, morpholine, or sulfamate) to non-polar (e.g. benzyl, p-fluorobenzyl, phenethyl, or p-fluorophenethyl). The substitution on phenyl ring was done either at para or meta position to investigate the impact of different positional isomerism on activity. Moreover, the imidazothiazole nucleus has been replaced with isosteric imidazooxazole to study the impact of this modification on activity. The target compounds were tested against a panel of 60 cancer cell lines from 9 different cancer types at 10 μM dose, then in 5-dose mode for the most active compounds to measure potency. Upon testing the most active molecules against a panel of kinases, a novel ErbB4 inhibitor with preferential activity and selectivity was discovered. Further testing on whole-cell kinase was performed to ensure the compound's ability to penetrate cell wall and inhibit ErbB4 kinase inside the cell. To measure safety and selectivity, the most active compounds were tested on normal cell line. Selectivity against ErbB4 kinase was discovered by serendipity upon testing the most active antiproliferative agents against a panel of kinases. Several tests were also conducted such as hERG to ensure safety as well as CYP 3A4 and 2D6 to measure enzyme inhibition. Docking and molecular dynamic simulation were also performed for the most active compound.

2. Results and discussion

2.1. Chemistry

Scheme 1 illustrates cyclization reaction between α-bromo-3(4)-methoxyacetophenone and 2-amino-thiazole (1) in refluxing ethanol to yield intermediates 2a,b [21]. Coupling of the intermediates 2a,b with 4-iodo-2-(methylthio)pyrimidine was carried out in presence of palladium(II) acetate as a catalyst,

triphenylphosphine as a ligand, and cesium carbonate to obtain compounds 3a,b. Reaction of compounds 3a,b with oxone resulted in oxidation of the methylsulfide moiety to sulfone (compounds 4a,b) [22,23]. Demethylation of the methoxy groups of compounds 4a,b was carried out using boron tribromide to obtain the corresponding hydroxyl analogues 5a,b. It is noteworthy that the hydroxyl products appeared on the TLC at higher R_f than the methoxy starting materials. This is unusual and unexpected but the identity of hydroxyl compounds 5a,b was confirmed by NMR and LC-MS analyses. This unusual finding was not encountered with the other hydroxyl intermediates 7a,b, 10, and 15. Finally, adding appropriate substituted alkyl halide or sulfamoyl chloride in presence of potassium carbonate or sodium hydride, respectively yielded the target derivatives Ia-p.

The target derivatives IIa-e and IIIa-e were synthesized by the pathway shown in Scheme 2. They were obtained through a pathway similar to that utilized for synthesis of compounds Ia-p (Scheme 1) but using either 4-iodopyrimidine or iodobenzene in the first step instead of 4-iodo-2-methylthiopyrimidine. Compound 6a could be synthesized by another method through removal of the mesyl group of 4b using sodium borohydride.

As shown in Scheme 3, interaction of compound 2b with 3-iodothioanisole was carried out under similar reaction conditions as utilized for synthesis of 3a,b and 6a,b to yield compound 8. Further oxidation of the methylthio group using oxone, demethylation of methoxy group, and subsequent alkylation of the resulting hydroxyl group similar to Schemes 1 and 2 led to formation of compounds IVa-e.

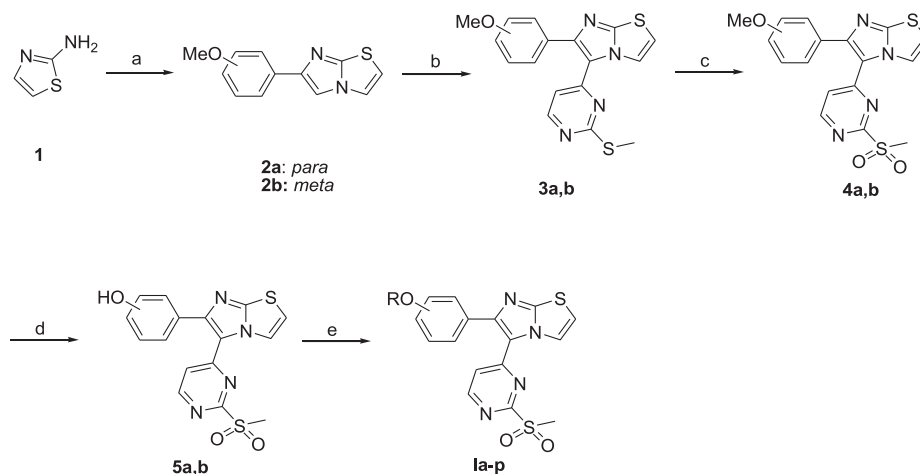Scheme 4 demonstrates the synthesis of target compounds Va,b. The synthetic steps were carried out similar to synthesis of compounds Ik and Il shown in Scheme 1. The methyl sulfide intermediate 13 was oxidized by oxone to the corresponding sulfone derivative 14 [24]. Demethylation of methoxy group in the next step followed by reaction with benzyl chloride or 4-fluorobenzyl chloride were carried out using the same reaction conditions shown in Schemes 1–3 to yield the target compounds Va,b. The exact structures of all the target compounds are illustrated in Tables 1 and 2.

2.2. Biological studies

2.2.1. Antiproliferative activity evaluation over NCI-60 cancer cell line panel

At the beginning of this study, we synthesized the target compounds Ia-p. In their structures, we introduced a variety of hydrophilic or hydrophobic moieties with positional isomers at para or meta positions to investigate their effects on activity. The target compounds Ia-p together with the methoxy intermediates 4a,b and the hydroxyl intermediate compounds 5a,b were tested for antiproliferative activity against NCI-60 cell line panel. The structures of each compound along with the mean growth percentages after treatment of the cell lines with each are illustrated in Table 1.

As per the results, it is obvious that meta-disubstituted phenyl at position 6 on the imidazothiazole nucleus is more favorable for activity than para-disubstituted analogues. The substituent at meta position maybe at proper orientation in the receptor site. In addition, hydrophobic substituents on that ring are more optimal than the hydrophilic ones. This can be rationalized that hydrophobic substituents at this location of the structure is required to interact with some hydrophobic pocket in the receptor site. Moreover, hydrophobic substituents increase the overall molecular hydrophobicity and ability to cross the cell membrane to increase cancer cellular exposure to the compound. Any or both of these effects can lead to enhanced antiproliferative activity of the molecules possessing hydrophobic substituent, especially Ik and Il. Compound Ik

Allitinib

Poziotinib

Dacomitinib

Lapatinib

Afatinib

Canertinib

Quinazoline derivatives

Neratinib

Pyrotinib

Quinoline derivatives

Ibrutinib

AC-480 (BMS-599626)

Other derivatives

The target compounds

R^1 = Substituted alkyl, sulfamoyl, (*p*-fluoro)benzyl, (*p*-fluoro)phenethyl, benzoylmethyl

R^2 = H, SO$_2$CH$_3$

X = S, O

Y = N, CH

Fig. 1. Structures of the reported pan-HER inhibitors and the target compounds.

Scheme 1. Reagents and reaction conditions: a) α-Bromo-3(4)-methoxyacetophenone, EtOH, reflux, 16 h, 80−85%; b) 4-Iodo-2-(methylthio)pyrimidine, Pd(OAc)$_2$, Cs$_2$CO$_3$, PPh$_3$, DMF, 80 °C, 12 h, 30−34%; c) Oxone, MeOH, H$_2$O, rt, 16 h, 80−85%; d) BBr$_3$, CH$_2$Cl$_2$, -78 °C, 1 h; rt, overnight, 55−60%; e) Appropriate substituted alkyl halide reagent or sulfamoyl chloride, K$_2$CO$_3$ (with alkyl halide) or NaH (with sulfamoyl chloride), anhydrous DMF, 0 °C then rt, 1−2 h, 20−60%.
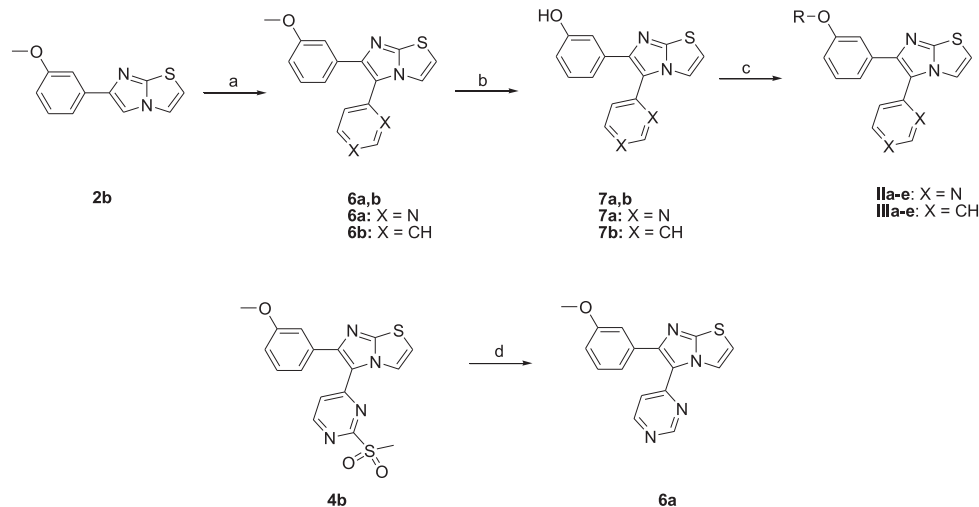
Scheme 2. Reagents and reaction conditions: a) 4-Iodopyrimidine or iodobenzene, Pd(OAc)$_2$, Cs$_2$CO$_3$, PPh$_3$, DMF, 80 °C, 12 h, 25−30%; b) BBr$_3$, CH$_2$Cl$_2$, -78 °C, 1 h; rt, overnight, 35−40%; c) Appropriate aralkyl halide reagent, K$_2$CO$_3$, anhydrous DMF, 0 °C then rt, 1−2 h, 30−55%; d) NaBH$_4$, MeOH/CH$_2$Cl$_2$ (1:1 v/v), rt, 2−3 h, 65%.
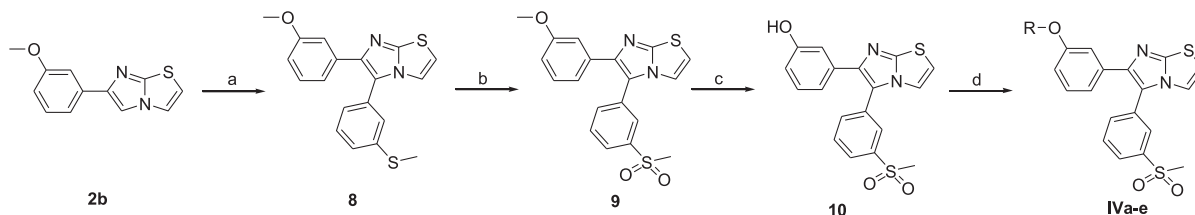
Scheme 3. Reagents and reaction conditions: a) 3-Iodothioanisole, Pd(OAc)$_2$, Cs$_2$CO$_3$, PPh$_3$, DMF, 80 °C, 12 h, 40%; b) Oxone, MeOH, H$_2$O, rt, 16 h, 78%; c) BBr$_3$, CH$_2$Cl$_2$, -78 °C, 1 h; rt, overnight, 40%; d) Appropriate aralkyl halide reagent, K$_2$CO$_3$, anhydrous DMF, 0 °C then rt, 1−2 h, 25−40%.

with unsubstituted benzyloxy is more active than **II** possessing *p*-fluorobenzyloxy, thus fluoro is not highly tolerated on the benzyl moiety. Extension of the spacer to have 2-atom distance between the oxygen and phenyl ring (such as compounds **Im** and **Io**) instead of one in case of compound **Ik** led to reduced activity. This linker elongation might lead to inappropriate fitting at the receptor site.

In the next phase of our study, we decided to retain *meta*-disubstituted phenyl at position 6 of the imidazothiazole nucleus

carrying hydrophobic substituent and start investigating the impact of structural modification of other parts of the structure on activity. We tried pyrimidine lacking mesyl group (compounds **6a**, **7a**, and **IIa-e**), mesylphenyl lacking the two nitrogen atoms (compounds **9**, **10**, and **IVa-e**), and unsubstituted phenyl lacking the two nitrogen atoms and the methylsulfonyl group (compounds **6b**, **7b**, and **IIIa-e**) at position 5 of the imidazothiazole scaffold. We also retained the mesylpyrimidinyl moiety and tried imidazooxazole
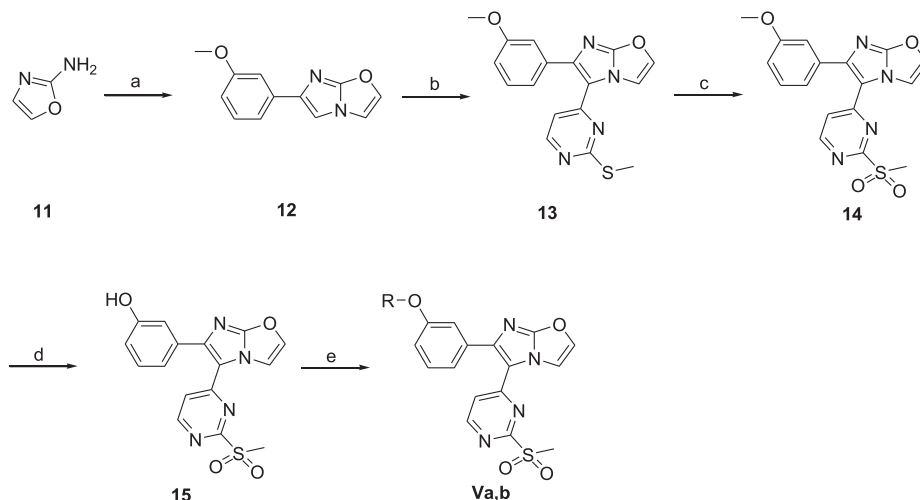
Scheme 4. Reagents and reaction conditions: a) α-Bromo-3-methoxyacetophenone, EtOH, reflux, 16 h, 80–85%; b) 4-Iodo-2-(methylthio)pyrimidine, Pd(OAc)$_2$, Cs$_2$CO$_3$, PPh$_3$, DMF, 80 °C, 12 h, 30%; c) Oxone, MeOH, H$_2$O, rt, 16 h, 65%; d) BBr$_3$, CH$_2$Cl$_2$, -78 °C, 1 h; rt, overnight, 15%; e) Benzyl chloride or 4-fluorobenzyl chloride, K$_2$CO$_3$, anhydrous DMF, 0 °C then rt, 1–2 h, 15% (**Va**), 20% (**Vb**).

Table 1
Structures of compounds **4a,b**, **5a,b**, and **Ia-p** and the mean growth percentage values of NCI-60 panel after treatment with each compound..
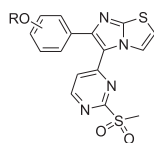
Compound No.	Position of OR	R	Mean Growth%[a]
4a	*Para*	Me	73.02%
4b	*Meta*	Me	NT[b]
5a	*Para*	H	99.74%
5b	*Meta*	H	90.04%
Ia	*Para*	Me$_2$N-(CH$_2$)$_2$-	102.24%
Ib	*Para*	(*i*-Pr)$_2$N-(CH$_2$)$_2$-	81.13%
Ic	*Para*		101.33%
Id	*Para*		100.87%
Ie	*Para*	Bn	95.11%
If	*Para*	Ph-(CH$_2$)$_2$-	91.15%
Ig	*Meta*	Me$_2$N-(CH$_2$)$_2$-	93.74%
Ih	*Meta*	(*i*-Pr)$_2$N-(CH$_2$)$_2$-	81.75%
Ii	*Meta*		94.15%
Ij	*Meta*		83.54%
Ik	*Meta*	Bn	**63.38%**
Il	*Meta*	4-Fluorobenzyl	**60.56%**
Im	*Meta*	Ph-(CH$_2$)$_2$-	95.99%
In	*Meta*	4-Fluorophenyl-(CH$_2$)$_2$-	91.58%
Io	*Meta*	PhCOCH$_2$	93.97%
Ip	*Meta*	SO$_2$NH$_2$	97.93%

[a] Calculated by dividing the summation of growth percentage values over the number of tested cell lines.
[b] Not selected by the NCI for testing over NCI-60 panel.

instead of imidazothiazole (compounds **14**, **15**, and **Va,b**). Their structures and mean growth percentage values of the NCI-60 panel after treatment with each compound are illustrated in Table 2. The results showed that imidazothiazole is more optimal for activity

Table 2
Structures of compounds **6a,b**, **7a,b**, **9**, **10**, **14**, **15**, and **IIa-e**, **IIIa-e**, **IVa-e**, and **Va,b** & their mean growth percentage values of NCI-60 panel after treatment with each compound..

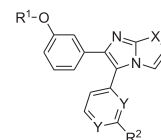| Compound No.	R^1	R^2	X	Y	Mean Growth%[a]
6a	Me	H	S	N	NT[b]
6b	Me	H	S	CH	96.64%
7a	H	H	S	N	85.46%
7b	H	H	S	CH	94.00%
9	Me	SO$_2$Me	S	CH	99.75%
10	H	SO$_2$Me	S	CH	99.19%
14	Me	SO$_2$Me	O	N	95.99%
15	H	SO$_2$Me	O	N	102.12%
IIa	Bn	H	S	N	78.42%
IIb	4-Fluorobenzyl	H	S	N	76.32%
IIc	Ph-(CH$_2$)$_2$-	H	S	N	96.44%
IId	4-Fluorophenyl-(CH$_2$)$_2$-	H	S	N	96.02%
IIe	PhCOCH$_2$	H	S	N	97.00%
IIIa	Bn	H	S	N	99.35%
IIIb	4-Fluorobenzyl	H	S	CH	97.82%
IIIc	Ph-(CH$_2$)$_2$-	H	S	CH	98.93%
IIId	4-Fluorophenyl-(CH$_2$)$_2$-	H	S	CH	87.46%
IIIe	PhCOCH$_2$	H	S	CH	84.63%
IVa	Bn	SO$_2$Me	S	CH	87.59%
IVb	4-Fluorobenzyl	SO$_2$Me	S	CH	74.68%
IVc	Ph-(CH$_2$)$_2$-	SO$_2$Me	S	CH	95.30%
IVd	4-Fluorophenyl-(CH$_2$)$_2$-	SO$_2$Me	S	CH	82.89%
IVe	PhCOCH$_2$	SO$_2$Me	S	CH	91.02%
Va	Bn	SO$_2$Me	O	N	101.42%
Vb	4-Fluorobenzyl	SO$_2$Me	O	N	89.69%

[a] Calculated by dividing the summation of growth percentage values over the number of tested cell lines.
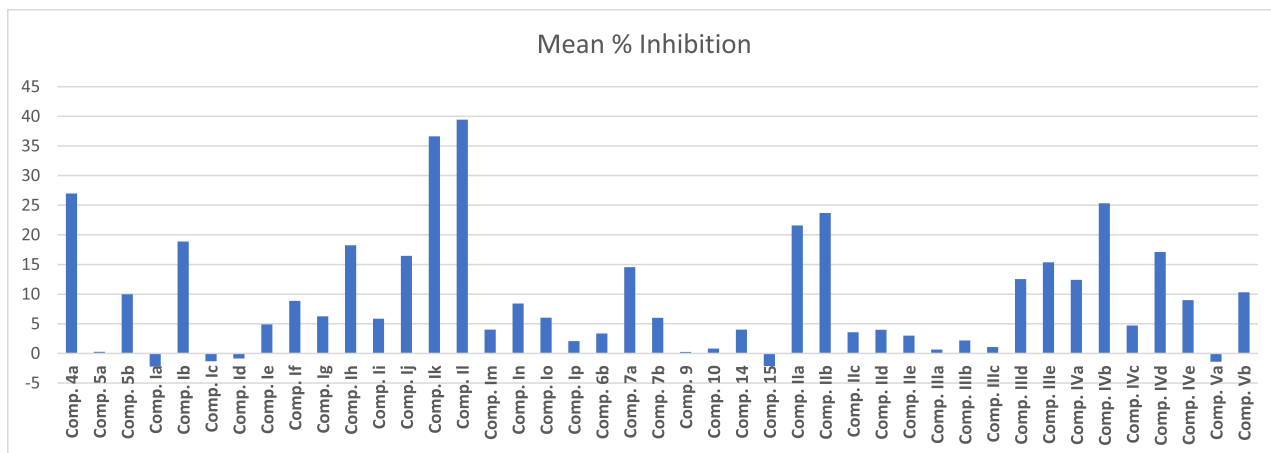[b] Not selected by the NCI for testing over NCI-60 panel.

Fig. 2. Mean inhibition percentage values of all the tested compounds against NCI-60 cancer cell line panel. The highest activity was reported with compounds **Ik** and **Il**.

than imidazooxazole. The higher hydrophobicity of sulfur compared to oxygen can lead to higher ability to cross the cell membrane and exert stronger antiproliferative activity. In addition, the loss of pyrimidine nitrogen atoms and/or methylsulfonyl group leads to weaker activity. They may synergize together to induce stronger activity against the molecular target(s). Fig. 2 summarizes the mean inhibition percentage values of all the tested compounds against NCI-60 panel.

Based on the NCI one-dose results, compounds **Ik** and **Il** were selected for further testing in 5-dose testing mode to calculate their IC$_{50}$ values. Both compounds were tested at 100, 10, 1, 0.1, and 0.01 μM concentrations. Their IC$_{50}$ values and inhibition percentage values at 10 μM concentration against the most sensitive cell lines of each cancer type are summarized in Tables 3 and 4. The results are compared with those of sorafenib (multikinase inhibitory anticancer drug) and ibrutinib (pan-HER inhibitory anticancer agent) as reference standards. In addition, the dose-response curves of compounds **Ik** and **Il** against all the tested cell lines are illustrated in Fig. 3.

The results indicate that both compounds **Ik** and **Il** exerted more promising antiproliferative activity than sorafenib. Compound **Ik** is more potent than sorafenib against seven out of nine cell lines. Similarly, Compound **Il** demonstrated higher potency than sorafenib against six cell lines. Compound **Ik** is more potent than

ibrutinib against six cell lines while **Il** showed higher potency than ibrutinib against five cell lines. The highest potency was recorded for compound **Ik** against SK-MEL-5 with sub-micromolar IC$_{50}$ value (0.51 μM). Upon testing against WI-38 normal cells, it is found that both compounds **Ik** and **Il** are relatively more selective toward cancer than normal cells.
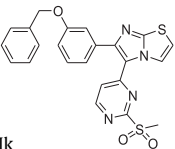
2.2.2. Kinase profiling

Based on our previous experience with imidazo[2,1-*b*]thiazole derivatives as inhibitors of RAF kinases [22,25], we initially tested the most promising antiproliferative compound **IK** and **Il** at 10 μM concentration against a small panel of nine kinases including RAF kinases and others (Table 5). Both compounds did not inhibit wild-type B-RAF or RAF1 significantly. Interestingly, both compounds exerted the highest inhibition percentage values against ErbB4 kinase (96.10% and 60.21%, respectively). In addition, compound **Ik** inhibited both EGFR and V600E-B-RAF with inhibition percentage values of 63.57% and 62.15%, respectively.

Subsequently, we decided to test compound **Ik** against an additional panel of 54 kinases, some of them are related to HER pathway and others belong to other kinase families to investigate its selectivity. The results are summarized in Fig. 4. At 10 μM concentration, it produced more than 50% inhibition against JAK3 and JNK3 kinases only (77.50% and 66.00%, respectively). However, its

Table 3
Antiproliferative activity of compound **Ik** against the most sensitive cell line of each cancer type & IC$_{50}$ values of sorafenib and ibrutinib against the same cell lines.

Cell line	Cancer type	Ik % inhibition at 10 μM	Ik IC$_{50}$ (μM)	Sorafenib (IC$_{50}$, μM)	Ibrutinib (IC$_{50}$, μM)
MOLT-4	Leukemia	73.53%	**1.02**	3.16	3.98
NCI−H522	Non-small cell lung cancer	94.09%	**4.91**	5.01	0.06
HCC-2998	Colon cancer	67.64%	**1.78**	3.16	15.85
U251	CNS cancer	10.94%	**6.08**	2.00	6.31
SK-MEL-5	Melanoma	99.86%	**0.51**	2.51	6.31
OVCAR-4	Ovarian cancer	26.22%	**3.78**	3.16	7.94
UO-31	Renal cancer	96.30%	**1.55**	2.51	1.26
DU-145	Prostate cancer	159.56%	**1.67**	3.16	2.00
MDA-MB-468	Breast cancer	165.07%	**1.04**	2.00	0.03
WI-38	*Normal cells*	*56.43%*	*8.54*	*NT*	*NT*

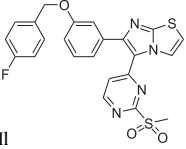Bold figures indicate stronger potency than sorafenib and/or ibrutinib.

Table 4

Antiproliferative activity of compound **Il** against the most sensitive cell line of each cancer type & IC$_{50}$ values of sorafenib and ibrutinib against the same cell lines.

Cell line	Cancer type	Il		Sorafenib (IC$_{50}$, μM)	Ibrutinib (IC$_{50}$, μM)
		% inhibition at 10 μM	IC$_{50}$ (μM)		
HL-60(TB)	Leukemia	56.33%	**3.36**	1.58	19.95
NCI−H322 M	Non-small cell lung cancer	NT%	**1.82**	2.51	0.10
HCC-2998	Colon cancer	116.25%	**1.76**	3.16	15.85
SNB-75	CNS cancer	4.08%	15.6	3.16	3.16
SK-MEL-5	Melanoma	94.61%	**1.54**	2.51	6.31
OVCAR-4	Ovarian cancer	34.91%	**3.98**	3.16	7.94
UO-31	Renal cancer	124.08%	**1.68**	2.51	1.26
DU-145	Prostate cancer	153.83%	**1.89**	3.16	2.00
MDA-MB-468	Breast cancer	163.64%	**1.80**	2.00	0.03
WI-38	*Normal cells*	*21.65%*	*12.64*	*NT*	*NT*

Bold figures indicate stronger potency than sorafenib and/or ibrutinib.
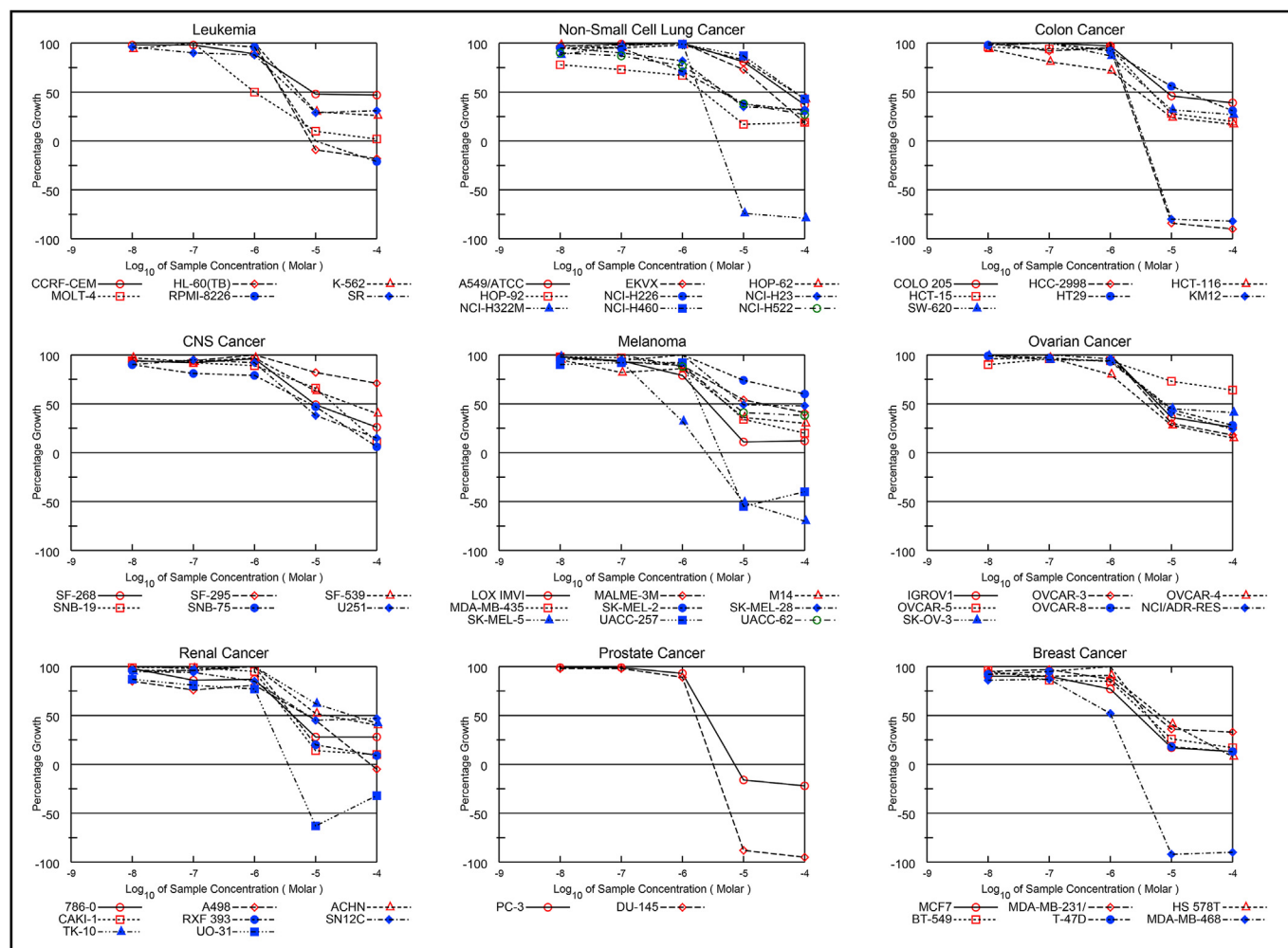
(A)

Fig. 3. Dose-response curves of compounds **Ik** (Fig. 3A) and **Il** (Fig. 3B) against the NCI-60 cell line panel of nine cancer types.

inhibition percentage values against the other tested kinases were less than 50%, i.e. the IC_{50} values against these kinases are higher than 10 μM.

As per the one-dose inhibition percentage values of compound **Ik**, it was further tested in a 10-dose assay against the three most inhibited kinases (EGFR, ErbB4, JAK3, JNK3, and V600E-B-RAF) to determine its IC_{50} values. The results are shown in Table 6. It exerted 2-digit nanomolar IC_{50} value (15.24 nM) against ErbB4 kinase, while its IC_{50} values against the other two kinases are in one-to two-digit micromolar scale. Compound **Ik** is 651-fold more selective toward ErbB4 kinase than EGFR (ErbB1), 548-fold more selective toward ErbB4 than JAK3, 341-fold more selective against ErbB4 than JNK3, and 866-fold more selective toward ErbB4 than V600E-B-RAF. Moreover, it is 9-fold more potent than staurosporine against ErbB4 kinase. These results indicate that we have discovered a relatively selective and potent ErbB4 kinase inhibitor.

According to the NCI-60 cell line results, compound **Ik** and **IIa** are the most active antiproliferative agents. Their IC_{50} values against ErbB4 were measured and compared. Despite of the minor structural difference between both compounds, the difference in potency is major. The fluorinated benzyl derivative **Il** is 47.2-fold less potent than the non-fluorinated analogue **Ik**. Therefore, fluoro substitution at *para* position on the benzyl moiety is not well tolerated. Docking studies were performed to explain this interesting difference in potency.

2.2.3. SAR against ErbB4

In order to study the relationship between ErbB4 inhibitory effect and the structures, all the target compounds **4a,b**, **5a,b**, **6a,b**, **7a,b**, **9**, **10**, **14**, **15**, **Ia-p**, **IIa-e**, **IIIa-e**, **IVa-e**, and **Va,b** were tested against ErbB4 kinase at 1 μM concentration. The inhibition percentage results are shown in Fig. 5.

Imidazothiazole nucleus is more optimal for activity against ErbB4 kinase than the isosteric imidazooxazole. The imidazothiazole derivatives **Ik**, **Il**, **4b**, and **5b** are significantly more active than the corresponding imidazooxazole analogues **Va**, **Vb**, **14**, and **15**.

In addition, the impact of the ring attached to position 5 of the imidazothiazole ring was studied. Unsubstituted phenyl (compounds **IIIa-e**) and mesylphenyl (**IVa-e**) are devoid of any promising ErbB4 kinase inhibition. However, pyrimidinyl (e.g. compounds **IIa-d**) and mesylpyrimidinyl (e.g. compounds **Ik** and **Il**) are much more active. The presence of both pyrimidinyl nitrogen atoms and methylsulfonyl group, or at least the pyrimidinyl nitrogen atoms, is essential for activity.

Moreover, we studied the impact of substituent at position 6 of the imidazothiazole nucleus on activity. Starting with the hydroxyl intermediates **5a,b**, **7a,b**, **10**, and **15**, they showed no promising inhibitory effect against ErbB4 kinase. Similarly, derivatives possessing hydrophilic substituents attached to the phenyl ring **Ia-d**, **Ig-j**, and **Ip** are not promising as well. Insertion of a small hydrophobic group such as methyl led to improvement of inhibitory effect. For example, the methoxy derivative **4b** is more active than the corresponding hydroxyl analogue **5b**. Bulkier, more hydrophobic substituents produced higher inhibitory effect against the kinase. The optimal substituent is benzyl (compounds **Ik** and **IIa** which are the most potent inhibitors of ErbB4 among this series). Substitution of benzyl with *p*-fluoro (compounds **Il** and **IIb**) led to significant reduction in kinase inhibitory effect. Extension of the methylene spacer of compounds **Ik** and **IIa** into ethylene (compounds **Im** and **IIc**) or −CH₂CO- (compounds **Io** and **IIe**) led to decreased activity. 4-Fluorophenethyl substituent (compounds **In** and **IId**) is also less

favorable for activity than unsubstituted benzyl. Furthermore, *meta*-disubstituted benzene at position 6 of the imidazothiazole nucleus (e.g. compounds **4b**, **5b**, **Ig-k**, and **Im**) is more favorable for activity than the corresponding *para*-disubstituted benzene analogues **4a**, **5a**, and **Ia-f**. This might affect the orientation inside the kinase active site and hence affinity and potency.

The most active compounds, **4b**, **Ik**, **Il**, and **IIa-d** were further tested in 10-dose assay to calculate their IC_{50} values against ErbB4 kinase. The highest potency was exerted by compounds **Ik** and **IIa** (15.24 and 17.70 nM, respectively) while the other compounds showed 3-digit nanomolar IC_{50} values. Based on these results, compounds **Ik** and **IIa** were selected for further studies.

Fig. 6 summarizes the key SAR aspects of this series of compounds as inhibitors of ErbB4 kinase and as antiproliferative agents.

2.2.4. Kinase profiling of compound IIa

Based on the SAR studies against ErbB4 kinase, compound **IIa** is the second most potent inhibitor. We decided to test it at 10 μM concentration against the same 63-kinase panel similar to compound **Ik** to investigate its kinase selectivity. The inhibition percentage values are illustrated in Fig. 7. At 10 μM, compound **IIa** exerted more than 60% inhibition against 12 kinases including ErbB4 and less than 60% inhibition against the other 51 kinases. It is noteworthy that compound **IIa** showed higher efficacy at 10 μM against ErbB4 than the most potent compound **Ik**.

After that, compound **IIa** was tested in 10-dose mode against the 12 most sensitive kinases to calculate its IC_{50} values. The results are summarized in Table 7. The compound exerted 2-digit nanomolar IC_{50} value against ErbB4 kinase only, 3-digit nanomolar IC_{50} values against EGFR (T790 M) and KDR only, and 4-digit nanomolar range IC_{50} values against the other nine kinases. The relative selectivity of compound **IIa** against ErbB4 kinase is obvious. For example, it is 21.5-fold more selective toward ErbB4 kinase than EGFR (T790 M), the second most sensitive kinase.
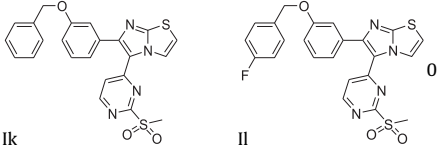
2.2.5. In-cell ErbB4 kinase assay

In order to investigate the capability of the most active antiproliferative compound **Ik** to cross the cell membrane and inhibit ErbB4 kinase inside the cells, it was tested against T-47D cell line that expresses endogenous ErbB4 [28]. T-47D cell line was treated with ten concentrations of compound **Ik** in a 3-fold serial dilution starting from 10 μM and lapatinib was utilized as a reference standard in this assay (IC_{50} of lapatinib = 190 nM). Compound **Ik** showed ability to penetrate the cell membrane and inhibit ErbB4 kinase inside the cells with IC_{50} value of 3.30 ± 0.05 μM. As per the results of compound **Ik** over the NCI-60 cell line panel (supplementary file), its IC_{50} value against T-47D cell line is 4.08 μM. Therefore, its IC_{50} value in whole-cell ErbB4 assay is less than its antiproliferative IC_{50} value, i.e. the compound inhibits more than 50% of the in-cell ErbB4 enzymatic activity at the antiproliferative IC_{50} concentration. It can be concluded that molecular mechanism of antiproliferative activity of compound **Ik** against T-47D cell line can be, at least partially, ErbB4 kinase inhibition.

2.2.6. hERG ion channel assay

The human ether-a-go-go related gene (hERG) is a gene reported to encode the inward rectifying voltage-gated potassium channels in the heart. Voltage-gated K^+ channels have a contribution in cardiac repolarization. hERG current inhibition prolongs the QT interval and results in fatal ventricular tachyarrhythmia, *Torsade de Pointes* [29−31]. The most promising compounds in this series,

Table 5
Inhibitory effects of compounds **Ik** and **Il** at 10 μM concentration against nine kinases.[a]

Kinase	Ik	Il
	% inhibition	% inhibition
B-RAF (wild-type)	34.33% ± 5.62%	9.62% ± 0.21%
c-SRC	−22.15% ± 0.91%	2.46% ± 1.52%
EGFR (HER1)	63.57% ± 1.26%	−5.54% ± 0.21%
ErbB2 (HER2)	2.75% ± 0.26%	−2.99% ± 0.53%
ErbB4 (HER4)	**96.10% ± 0.37%**	**60.21% ± 0.14%**
FGFR1	3.33% ± 0.38%	−0.04% ± 0.04%
KDR (VEGFR2)	24.78% ± 0.09%	24.77% ± 0.07%
RAF1	23.00% ± 0.43%	10.82% ± 2.78%
V600E-B-RAF	62.15% ± 0.84%	33.56% ± 2.19%

[a] The results are expressed as means of duplicate assays ± S.E.M. ATP concentration is 1 μM.

Ik and **IIa**, were tested against hERG. E−4031 was also examined as a positive control. The assay principle depends on the competition of fluorescent-labeled tracer binding to a membrane preparation possessing hERG. The IC$_{50}$ values of compounds **Ik**, **IIa**, and E−4031 against hERG are 12,410, 12,830, and 24.2 nM, respectively (Table 8). So compounds **Ik** and **IIa** are 513-fold and 530-fold, respectively, safer than E−4031 against hERG. These results show also that compound **Ik** will be devoid of significant cardiotoxicity at its IC$_{50}$ values against the most sensitive cancer cell lines.

2.2.7. Testing against CYP 2D6 and 3A4

Azoles are known for ability to inhibit cytochrome P450 isoenzymes. Our target compounds possess azole moiety as a part of the imidazo[2,1-*b*]thiazole nucleus. In this assay, we decided to test compounds **Ik** and **IIa** against two of the major cytochrome P450 isozymes; CYP 2D6 and 3A4 to measure their IC$_{50}$ values as inhibitors. They were compared with ketoconazole, an azole-based antifungal agent known as inhibitor of CYP [32,33]. The results are shown in Table 9. Compounds **Ik** and **IIa** are much weaker than ketoconazole against both CYP 2D6 and 3A4. Compounds **Ik** and **IIa** are more than 10.8-fold less potent than ketoconazole against CYP 2D6. Similarly, they 7479-fold and 8786-fold, respectively, less potent against CYP 3A4 than ketoconazole. Therefore, there is no risk of significant CYP inhibition encountered with compounds **Ik** or **IIa**.

Table 6
IC$_{50}$ values of compound **Ik** and staurosporine (reference standard) against EGFR, ErbB4, and V600E-B-RAF kinases.[a]

Kinase	Compound Ik IC$_{50}$ (nM)	Staurosporine IC$_{50}$ (nM)
EGFR (HER1)	9920 ± 5.0	39.80 ± 1.2
ErbB4 (HER4)	**15.24** ± 0.8	138.00 ± 3.0
JAK3	8353 ± 2.0	8.00 ± 0.2
JNK3	5199 ± 3.0	73.10 ± 0.6
V600E-B-RAF	13200 ± 9.0	8.80 ± 1.1

[a] The results are expressed as means of duplicate assays ± S.E.M. ATP concentration is 1 μM.

2.2.8. Docking and molecular dynamic simulation

Compounds **Ie**, **Ik**, **Il**, **Im**, **IIa**, **IIb**, **IIc**, **IId**, **IIIa**, **IVa**, and **Va** were subjected to molecular docking analysis so that to gain deeper insight about their binding modes and the interactions occurred at the level of enzyme active site, where such study would allow for better understanding of the structure-activity relationship and the observed variations in the biological activities.

According to the results of docking study, our compounds appeared to adapt three binding conformations within the enzyme active site that are dependent on the structural variations in each compound (Fig. 8). The most potent compound **Ik** is able to establish three H-bond interactions within the ErbB4 enzyme active site; the first one between its imidazothiazole nitrogen and the Lys751 amino acid residue (N ….HN, 2.2 Å), the second interaction is between its pyrimidinyl nitrogen atom and the Met799 residue (N ….HN, 2.8 Å), while the mesyl group oxygen atom is able to secure the third H-bond with the corresponding Cys803 residue (O ….HS, 2.0 Å) (Fig. 9a). Compound **Il** appeared to establish the same network of interactions as that of **Ik**, however, the presence of fluorine substituent on the terminal benzyl moiety appeared to be inferior to the biological activity, which could be attributed to the local hydrophobic nature of the binding pocket and to the close proximity of fluorine atom to the Phe862 amino acid residue (Fig. 9b). In the absence of mesyl group as in compounds **IIa** and **IIb** the structures are able to form two H-bonds instead of three when compared to the most potent compound (Fig. 9c & d). Replacing the pyrimidine ring with benzene and/or removal of mesyl group as in the case of compounds **IVa** and **IIIa**, respectively appeared to lead to less favorable binding, since such structures would lose their ability to form H-bonding with the corresponding Met799 and Cys803 residue as observed earlier with the most potent compound (Fig. 9e & f). Structural modifications that involve *para*-substitution instead of *meta* (the case of compound **Ie**) or replacing benzyl moiety with phenethyl (the case of compound **Im**) while keeping the mesyl group lead to similar consequences; 1) Both structures adapt slightly different binding conformation compared to the most

Fig. 4. Mean inhibition percentage values of compound **Ik** against the 63 tested kinases at 10 μM concentration. The values are means of duplicate experiments.

Fig. 5. Mean inhibition percentage values of all the target compounds against ErbB4 at 1 μM concentration.

Fig. 6. Summary of SAR of the target compounds against ErbB4 kinase and NCI-60 cancer cell line panel.

potent compound, 2) Both structures share the same network of H-bond interactions that involves new engagement with Arg847 amino acid residue (Figs. 8,9g & 9h). Total loss of hydrogen bond interactions are associated with derivatives exhibiting extended phenethyl arm while lacking mesyl group as the case of compounds; **IIc** and **IId** (Fig. 9i & j). Finally, replacing the imidazothiazole core scaffold with imidazooxazole as in the case of compound **Va** would yield the third observed binding conformation (Fig. 8) and would produce change in the binding interactions with new involvement of Thr860 amino acid residue (Fig. 9k).

Since the ErbB enzymes are known for their conformational plasticity, especially in the kinase domain [34,35], we were interested in exploring the network of interactions occurred between our most potent compound **Ik** and the ErbB4 active site under dynamic motion. For the purpose, 50 ns molecular dynamic

simulation was carried out. The root-mean-squared deviations (RMSD) were utilized to assess system stability, where an adequate enzyme-ligand system equilibration was achieved within 6 ns from the beginning of the run and remained stable during the rest of the simulation time (Fig. 10).

Results of the dynamic simulation are consistent with the previously described docking binding mode; however, the results clearly demonstrated the pivotal role of the methylsulfonyl pyrimidinyl moiety in anchoring the enzyme active site, in which the mesyl group oxygen is involved in direct H-bond interaction with the Met799 residue for about 60% of the simulation time, while the pyrimidinyl nitrogen is engaged with the same residue for about 49% of the simulation time (Fig. 11). Indirect H-bond interactions (water-bridges) are observed between Lys751 and the corresponding imidazothiazole nitrogen and the benzyloxy oxygen for a
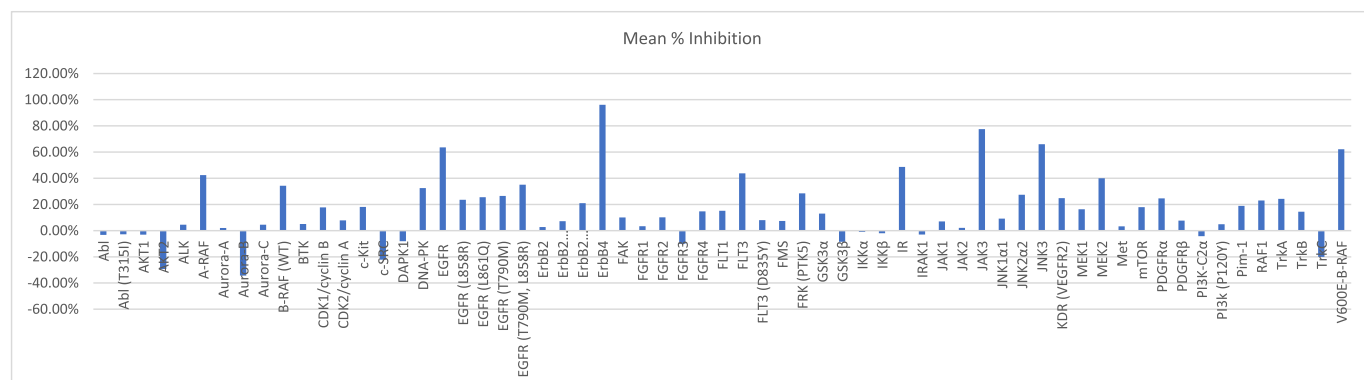

Fig. 7. Mean inhibition percentage values of compound **IIa** against the 63 tested kinases at 10 μM concentration. The values are means of duplicate experiments.

Table 7
IC$_{50}$ values (nM) of compound **IIa** against the most sensitive kinases.

Kinase	IC$_{50}$ (nM)[a]
A-RAF	7058 ± 4.0
B-RAF (wild-type)	1000 ± 5.0
EGFR (L861Q)	4354 ± 3.0
EGFR (T790 M)	380 ± 2.0
EGFR (T790 M, L858R)	8560 ± 4.0
ErbB4	**17.70** ± 0.3
FLT3	1362 ± 3.5
JNK3	5718 ± 7.0
KDR	710 ± 1.2
MEK2	3246 ± 2.0
RAF1	2028 ± 2.0
V600E-B-RAF	1587 ± 4.0

[a] The results are expressed as means of duplicate assays ± S.E.M. ATP concentration is 1 μM.

Table 8
IC$_{50}$ values of compounds **Ik**, **IIa**, and the reference standard compound **E-4031** over hERG.

Compound	IC$_{50}$ (nM) against hERG potassium ion channels[a]
Ik	12410 ± 12
IIa	12830 ± 8
E-4031 (reference standard)	24.20 ± 0.002

[a] The results are expressed as means of duplicate assays ± S.E.M.

Table 9
IC$_{50}$ values of compounds **Ik**, **IIa**, and the reference standard ketoconazole against Cytochrome P450 2D6 and 3A4 isozymes.

Compound	IC$_{50}$ (nM)[a]	
	CYP 2D6	CYP 3A4
Ik	**>90000**	**17800** ± 4
IIa	**>90000**	**20910** ± 6
Ketoconazole (reference standard)	**8310** ± 2	**2.38** ± 0.2

[a] The results are expressed as means of duplicate assays ± S.E.M.

period of 22% and 49%, respectively.

A new interaction is revealed represented by the ability of benzyloxy oxygen to water-bridge the Asp861 for a period of 37% of the simulation time. Furthermore, the dynamic results emphasized the contribution of the benzyl terminal to the overall binding, where it is able to establish significant hydrophobic interaction with the corresponding Phe862 for about 70% of the simulation time.

3. Conclusion

This study reports the discovery of first-in-class selective inhibitor of ErbB4 kinase that possesses imidazo[2,1-*b*]thiazole nucleus. SAR demonstrated that imidazo[2,1-*b*]thiazole is more optimal for activity than the isosteric imidazo[2,1-*b*]oxazole analogue. The presence of mesyl-substituted pyrimidine ring at position 5 of the imidazothiazole nucleus is crucial for activity. The presence of two nitrogen atoms of the pyrimidine ring together with methylsulfonyl group is synergistic for activity. At least the pyrimidine ring is essential for activity. Insertion of phenyl or mesylphenyl instead led to reduction of the activity against the cancer cell lines and ErbB4 kinase. Moreover, the presence of phenyl ring at position 6 of the imidazothiazole scaffold carrying benzyloxy substituent at *meta* position is the best for activity (e.g. compounds **Ik** and **IIa**). This study ended up with novel lead compounds, **Ik** and **IIa**, that are relatively preferential for ErbB4 kinase with IC$_{50}$ values of 15.24 and 17.70 nM, respectively. Although compound **Ik** is slightly more potent than **IIa**, compound **IIa** is more efficacious against ErbB4 kinase at 1 and 10 μM concentrations. Upon testing against 63-kinase panel, both compounds showed superior selectivity against ErbB4. Compound **Ik** exerted promising antiproliferative activity with promising potency against different cancer cell lines. Its IC$_{50}$ values ranges from sub-micromolar to one-digit micromolar range. In whole-cell kinase assay in T-47D breast cancer cell line, it showed ability to penetrate the cell membrane and inhibit ErbB4 kinase inside the cells at IC$_{50}$ value comparable to that against the same cell line in the antiproliferative testing. The biological results and SAR were supported
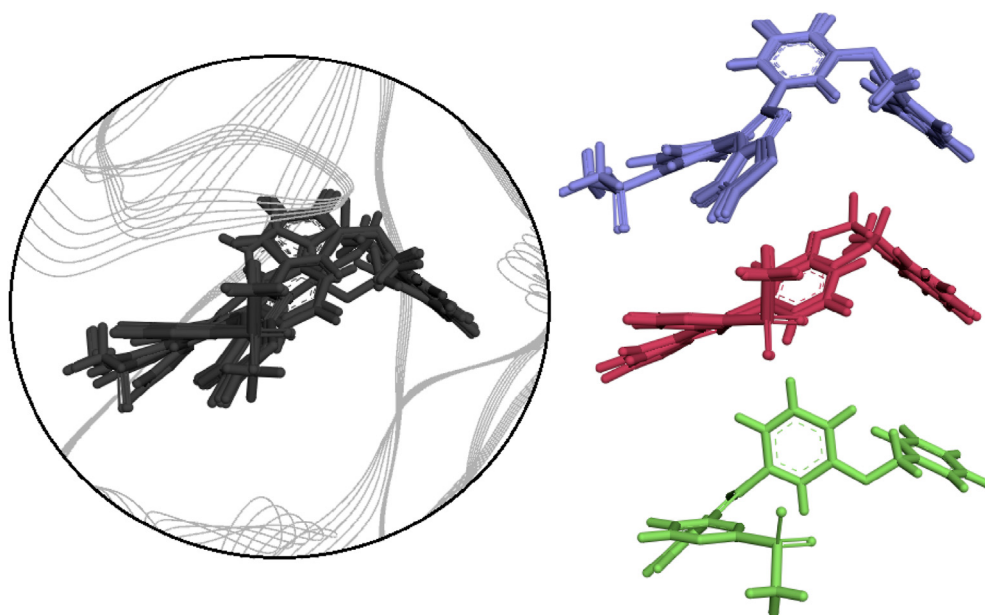

Fig. 8. Overlay and binding conformations for the compounds under study within the ErbB4 enzyme active site (PDB ID: 2R4B). Compounds **Ik**, **Il**, **IIa**, **IIb**, **IIIa**, **IVa** are illustrated in purple; while compounds **Ie**, **Im**, **IIc**, **IId** are illustrated in magenta, and compound **Va** in green colour.
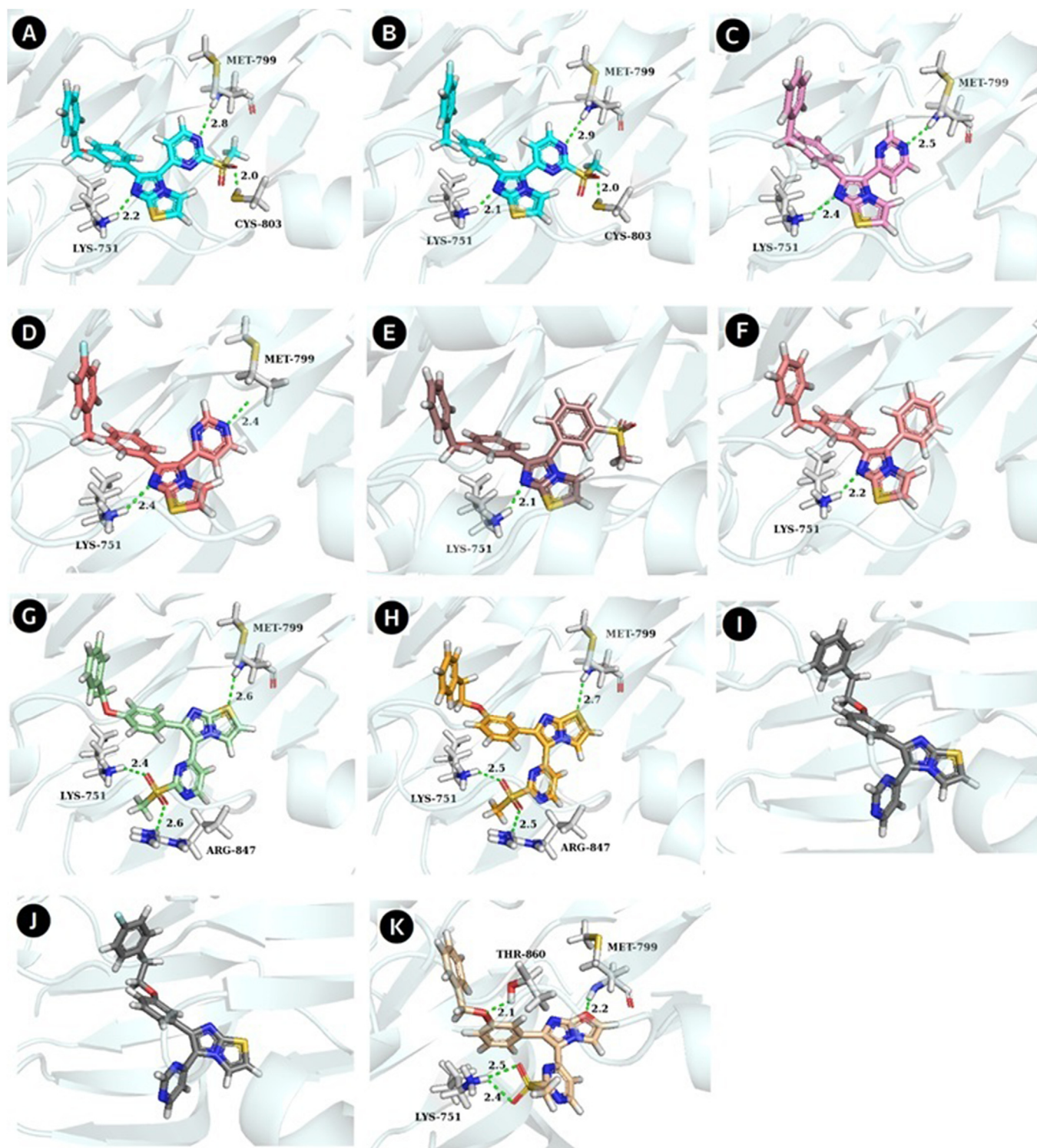
Fig. 9. Best-docked poses and interactions of compounds **Ik**, **Il**, **IIa**, **IIb**, **IVa**, **IIIa**, **Ie**, **Im**, **IIc**, **IId** and **Va** (respectively a-k) within the ErbB4 active site (PDB ID: 2R4B). The enzyme is represented in ribbon style. Green dashed lines represent hydrogen bond interactions while important amino acid residues are in sticks rendering.

by molecular docking and dynamic simulation studies. Furthermore, compound **Ik** possesses additional advantages such as high selectivity against cancer cells than normal cells, very weak inhibitory effect against hERG ion channels, and very weak potency as inhibitor of CYP 3A4 and 2D6 isozymes. The most potent ErbB4 inhibitors among this series, compounds **Ik** and **IIa** are the first selective ErbB4 kinase inhibitors to be reported in the scientific

literature. They can be useful tools for scientists working on ErbB4-related pathways who need selective ErbB4 inhibitor in their studies.

Further lead optimization will be carried out shortly. It is planned to replace the methylsulfonyl group with other substituents, optimize the benzyloxy moiety, and investigate the impact of substituted or fused imidazothiazole nucleus on activity. Further

Fig. 10. Plot of the protein-ligand root-mean-square-deviation (RMSD) values over the 50 ns simulation time for the ErbB4 enzyme Cα-atoms (blue) and compound **Ik** heavy atoms (red).

biological studies will be conducted accordingly.

4. Methods

4.1. General

Bruker Avance (300, 400, and 500 MHz spectrometers) were used to analyze the compounds by ^{1}H and ^{13}C NMR. LC-MS analysis was carried out by LC-MS analyzer (Waters Corporation, MA, USA). All the solvents and reagents were purchased from commercial companies and used as such. The final and intermediate compounds were purified by flash column chromatography (silica gel, pore size 0.040−0.063 mm, 230−400 mesh) using laboratory reagent grade solvents. Purity of the final compounds was confirmed to be >96% by elemental microanalysis.

4.2. Chemical synthesis

4.2.1. Synthesis of the methoxy intermediate compounds **4a,b**, **6a,b**, **9**, and **14**

It was accomplished using the reported procedure [21−23].

4.2.2. Alternative method for synthesis of compound **6a** from the methylsulfonyl analogue **4b**

To a stirred solution of compound **4b** (386 mg, 1 mmol) in methanol/dichloromethane (1:1 *v/v*) (10 mL) was added NaBH$_4$ (95 mg, 2.5 mmol) portionwise slowly at room temperature. The resultant solution was stirred at room temperature for 2−3 h. After

completion of reaction, the reaction mixture was quenched with saturated NaHCO$_3$ solution followed by water and the extracted with dichloromethane (3 × 10 mL). Combined organics were dried over anhydrous Na$_2$SO$_4$, filtered, and concentrated under vacuo to get crude compound. The crude compound was purified by silica gel column chromatography using ethyl acetate:hexane (3:7 *v/v*) as an eluent to afford desired compound which was confirmed by spectral analysis. Yield is 65%.

4.2.3. 6-(4-Methoxyphenyl)-5-(2-(methylsulfonyl)pyrimidin-4-yl) imidazo[2,1-b]thiazole (**4a**)

Purified by normal phase column chromatography, eluent hexane:ethyl acetate 85:15 *v/v* followed by 50:50 *v/v*; Yield: 80%; ^{1}H NMR (CDCl$_3$, 400 MHz) δ 8.88 (d, 1H, J = 4.5 Hz), 8.48 (d, 1H, J = 5.6 Hz), 7.57−7.55 (m, 2H), 7.40 (d, 1H, J = 5.7 Hz), 7.05−7.02 (m, 3H), 3.90 (s, 3H), 3.37 (s, 3H); ^{13}C NMR (DMSO-d_6, 75 MHz) δ 165.9, 160.4, 158.5, 157.0, 153.8, 152.3, 130.8 (2C), 126.6, 122.5, 119.3, 118.2, 115.8, 114.8 (2C), 55.7, 39.1; LC/MS *m/z*: 387.36 (M$^+$ + 1); CHN analysis: calculated C:52.84%, H:3.65%, N:14.50%; found: C:52.68%, H:3.58%, N:14.63%.

4.2.4. 6-(3-Methoxyphenyl)-5-(2-(methylsulfonyl)pyrimidin-4-yl) imidazo[2,1-b]thiazole (**4b**) [23]

Purified by normal phase column chromatography, eluent hexane:ethyl acetate 85:15 *v/v* followed by 50:50 *v/v*; Yield: 85%; ^{1}H NMR (CDCl$_3$, 300 MHz) δ 8.80 (d, 1H, J = 4.5 Hz), 8.50 (d, 1H, J = 5.6 Hz), 7.40−7.32 (m, 2H), 7.18 (dd, 2H, J = 0.9 and 1.5 Hz), 7.08−7.02 (m, 2H), 3.85 (s, 3H), 3.37 (s, 3H); ^{13}C NMR (CDCl$_3$, 75 MHz) δ 165.7, 162.3, 160.1, 157.5, 156.8, 153.2, 135.4, 130.2, 123.3, 121.3, 119.6, 117.7, 115.6, 114.1, 113.9, 55.5, 39.3; LC/MS *m/z*: 387.29 (M$^+$ + 1); CHN analysis: calculated C:52.84%, H:3.65%, N:14.50%; found: C:52.91%, H:3.68%, N:14.40%.

4.2.5. 6-(3-Methoxyphenyl)-5-(pyrimidin-4-yl)imidazo[2,1-b] thiazole (**6a**)

Purified by normal phase column chromatography, eluent hexane:ethyl acetate 80:20 *v/v* followed by 50:50 *v/v*; Yield: 25%; ^{1}H NMR (CDCl$_3$, 400 MHz) δ 9.18 (s, 1H), 8.73 (d, 1H, J = 4.4 Hz), 8.43 (d, 1H, J = 5.2 Hz), 7.37 (t, 1H, J = 8.0 Hz), 7.27 (d, 1H, J = 5.6 Hz), 7.20−7.18 (m, 2H), 7.01−6.97 (m, 2H), 3.83 (s, 3H); ^{13}C NMR (CDCl$_3$, 75 MHz) δ 165.6, 162.2, 160.0, 157.3, 156.7, 153.1, 135.2, 130.1, 123.2, 121.2, 119.5, 117.6, 115.6, 114.2, 113.8, 55.6; LC/MS *m/z*: 309.15 (M$^+$ + 1); CHN analysis: calculated C:62.32%, H:3.92%, N:18.17%; found: C:62.43%, H:3.88%, N:18.02%.

Fig. 11. Protein-ligand interaction over the 50 ns simulation period; **(a)** The fractions of interaction occurred between compound **Ik** and the ErbB4 enzyme. **(b)** 2D-ligand interaction diagram of compound **Ik** within the ErbB4 active site.

4.2.6. 6-(3-Methoxyphenyl)-5-phenylimidazo[2,1-b]thiazole (6b)

Purified by normal phase column chromatography, eluent hexane:ethyl acetate 80:20 v/v followed by 50:50 v/v; Yield: 30%; ^{1}H NMR (CDCl$_3$, 400 MHz) δ 9.16 (s, 1H), 8.71 (d, 1H, J = 4.5 Hz), 8.41 (d, 1H, J = 5.2 Hz), 7.35 (t, 1H, J = 8.0 Hz), 7.28 (d, 1H, J = 5.5 Hz), 7.18−7.15 (m, 3H), 7.00−6.96 (m, 3H), 3.84 (s, 3H); ^{13}C NMR (CDCl$_3$, 75 MHz) δ 165.5, 162.1, 159.9, 157.2, 156.6, 153.0, 135.1, 130.0, 123.2, 121.1, 119.4, 117.5, 115.5, 114.1, 113.6, 55.5; LC/MS m/z: 307.1 (M$^+$ + 1); CHN analysis: calculated C:70.56%, H:4.61%, N:9.14%; found: C:70.40%, H:4.77%, N:8.98%.

4.2.7. 6-(3-Methoxyphenyl)-5-(3-(methylsulfonyl)phenyl)imidazo [2,1-b]thiazole (9)

Purified by normal phase column chromatography, eluent hexane:ethyl acetate 80:20 v/v followed by 50:50 v/v; Yield: 78%; ^{1}H NMR (CDCl$_3$, 400 MHz) δ 9.17 (s, 1H), 8.72 (d, 1H, J = 4.6 Hz), 8.42 (d, 1H, J = 5.6 Hz), 7.37 (t, 1H, J = 8.0 Hz), 7.29 (d, 1H, J = 5.5 Hz), 7.20−7.17 (m, 3H), 7.01−6.97 (m, 2H), 3.84 (s, 3H), 3.37 (s, 3H); ^{13}C NMR (CDCl$_3$, 75 MHz) δ 165.6, 162.2, 159.8, 157.3, 156.7, 153.1, 135.2, 130.2 (2C), 123.3, 121.2, 119.5, 117.6, 115.6, 114.2, 113.8 (2C), 55.6, 39.2; LC/MS m/z: 385.0 (M$^+$ + 1); CHN analysis: calculated C:59.35%, H:4.19%, N:7.29%; found: C:59.46%, H:4.13%, N:7.20%.

4.2.8. 6-(3-Methoxyphenyl)-5-(2-(methylsulfonyl)pyrimidin-4-yl) imidazo[2,1-b]oxazole (14)

Purified by normal phase column chromatography, eluent hexane:ethyl acetate 80:20 v/v followed by 50:50 v/v; Yield: 65%; ^{1}H NMR (CDCl$_3$, 400 MHz) δ 8.50 (d, 1H, J = 6.0 Hz), 8.43 (d, 1H, J = 2.0 Hz), 7.55 (d, 1H, J = 2.0 Hz), 7.46 (d, 1H, J = 5.6 Hz), 7.41 (t, 1H, J = 8.0 Hz), 7.22−7.18 (m, 2H), 7.06−7.03 (m, 1H), 3.86 (s, 3H), 3.36 (s, 3H); ^{13}C NMR (CDCl$_3$, 100 MHz) δ 165.8, 162.4, 160.2, 157.6, 156.9, 153.4, 135.5, 130.4, 123.5, 121.4, 119.8, 117.8, 115.7, 114.3, 114.0, 55.6, 39.4; LC/MS m/z: 371.1 (M$^+$ + 1); CHN analysis: calculated C:55.13%, H:3.81%, N:15.13%; found: C:55.20%, H:3.75%, N:15.04%.

4.3. Demethylation of methoxy intermediates and synthesis of hydroxyl compounds 5a,b, 7a,b, 10, and 15

To a solution of compound 4a,b, 6a,b, 9, or 14 (0.1 mmol) in dry methylene chloride (1 mL), BBr$_3$ (0.04 mL of 1 M solution in dichloromethane, 0.6 mmol) was added dropwise at −78 °C under nitrogen. The mixture was allowed to stir at the same temperature for 30 min then at room temperature overnight. The reaction mixture was quenched and alkalinized using saturated aqueous Na$_2$CO$_3$. Ethyl acetate (10 mL) was added and the organic layer was separated. The aqueous layer was extracted with ethyl acetate (3 × 5 mL). The combined organic layer extract was washed with saturated saline and dried by anhydrous sodium sulfate. After evaporation of the solvent in vacuo, the residue was purified by normal phase column chromatography using hexane:ethyl acetate system as eluent.

4.3.1. 4-(5-(2-(Methylsulfonyl)pyrimidin-4-yl)imidazo[2,1-b] thiazol-6-yl)phenol (5a)

Purified by normal phase column chromatography, eluent hexane:ethyl acetate 80:20 v/v followed by 50:50 v/v; Yield: 55%; ^{1}H NMR (DMSO-d_6, 400 MHz) δ 9.86 (brs, 1H), 8.43−8.39 (m, 2H), 7.54−7.52 (m, 1H), 7.44−7.42 (m, 2H), 7.21 (d, 1H, J = 1.8 Hz), 6.89−6.87 (m, 2H), 3.40 (s, 3H); ^{13}C NMR (DMSO-d_6, 100 MHz) δ 159.5, 158.8, 158.3, 153.4, 152.4, 130.8 (2C), 125.0, 122.1, 118.7, 116.1 (2C), 115.4, 115.1, 39.3; LC/MS m/z: 373.24 (M$^+$ + 1); CHN analysis: calculated C:51.60%, H:3.25%, N:15.04%; found: C:51.40%, H:3.18%, N:15.12%.

4.3.2. 3-(5-(2-(Methylsulfonyl)pyrimidin-4-yl)imidazo[2,1-b] thiazol-6-yl)phenol (5b)

Purified by normal phase column chromatography, eluent hexane:ethyl acetate 80:20 v/v followed by 50:50 v/v; Yield: 60%; ^{1}H NMR (DMSO-d_6, 400 MHz) δ 9.67 (brs, 1H), 8.43−8.37 (m, 2H), 7.62 (d, 1H, J = 6.3 Hz), 7.58−7.49 (m, 2H), 6.99−6.86 (m, 3H), 3.44 (s, 3H); ^{13}C NMR (DMSO-d_6, 75 MHz) δ 162.3, 159.5, 158.1, 153.4, 152.4, 151.9, 135.6, 130.4, 122.0, 120.0, 119.1, 116.6, 116.1, 115.7, 115.5, 39.1; LC/MS m/z: 373.24 (M$^+$ + 1); CHN analysis: calculated C:51.60%, H:3.25%, N:15.04%; found: C:51.48%, H:3.33%, N:14.84%.

4.3.3. 3-(5-(Pyrimidin-4-yl)imidazo[2,1-b]thiazol-6-yl)phenol (7a)

Purified by normal phase column chromatography, eluent hexane:ethyl acetate 80:20 v/v followed by 50:50 v/v; Yield: 35%; ^{1}H NMR (DMSO-d_6, 500 MHz) δ 9.61 (s, 1H), 9.22 (d, 1H, J = 1.5 Hz), 8.63−8.60 (m, 2H), 7.49 (d, 1H, J = 4.5 Hz), 7.28 (t, 1H, J = 8.0 Hz), 7.25 (dd, 1H, J = 1.5, 5.5 Hz), 7.01−7.00 (m, 2H), 6.87−6.85 (m, 1H); ^{13}C NMR (DMSO-d_6, 125 MHz) δ 158.6, 157.6, 156.7, 155.3, 152.0, 149.7, 135.5, 129.9, 121.9, 119.7, 119.4, 116.8, 115.8, 115.5, 114.7; LC/MS m/z: 295.02 (M$^+$ + 1); CHN analysis: calculated C:61.21%, H:3.42%, N:19.04%; found: C:61.37%, H:3.29%, N:18.95%.

4.3.4. 3-(5-Phenylimidazo[2,1-b]thiazol-6-yl)phenol (7b)

Purified by normal phase column chromatography, eluent hexane:ethyl acetate 80:20 v/v followed by 50:50 v/v; Yield: 40%; ^{1}H NMR (DMSO-d_6, 500 MHz) δ 7.93 (d, 1H, J = 4.5 Hz), 7.59−7.53 (m, 6H), 7.18 (t, 1H, J = 8.0 Hz), 6.94−6.90 (m, 2H), 6.79 (d, 1H, J = 8.0 Hz); ^{13}C NMR (DMSO-d_6, 125 MHz) δ 157.6, 147.1, 136.5, 130.9, 129.8, 129.6 (2C), 129.4 (2C), 127.4, 122.9, 119.5, 118.2, 117.3, 115.8, 114.3; LC/MS m/z: 293.03 (M$^+$ + 1); CHN analysis: calculated C:69.84%, H:4.14%, N:9.58%; found: C:69.76%, H:4.06%, N:9.70%.

4.3.5. 3-(5-(3-(Methylsulfonyl)phenyl)imidazo[2,1-b]thiazol-6-yl) phenol (10)

Purified by normal phase column chromatography, eluent hexane:ethyl acetate 80:20 v/v followed by 50:50 v/v; Yield: 40%; ^{1}H NMR (DMSO-d_6, 500 MHz) δ 9.42 (brs, 1H), 7.98−7.96 (m, 2H), 7.86−7.84 (m, 2H), 7.78 (t, 1H, J = 7.5 Hz), 7.38 (d, 1H, J = 4.5 Hz), 7.10 (t, 1H, J = 8.0 Hz), 6.97 (s, 1H), 6.89 (d, 1H, J = 7.5 Hz), 6.67 (dd, 1H, J = 1.5, 8.0 Hz), 3.23 (s, 3H); ^{13}C NMR (DMSO-d_6, 125 MHz) δ 157.3, 149.0, 143.3, 141.6, 135.1, 133.9, 131.0, 130.5, 129.4, 127.2, 126.5, 120.8, 118.6, 118.1, 114.5, 114.2 (2C), 43.5; LC/MS m/z: 371.0 (M$^+$ + 1); CHN analysis: calculated C:58.36%, H:3.81%, N:7.56%; found: C:58.40%, H:3.70%, N:7.61%.

4.3.6. 3-(5-(2-(Methylsulfonyl)pyrimidin-4-yl)imidazo[2,1-b] oxazol-6-yl)phenol (15)

Purified by normal phase column chromatography, eluent hexane:ethyl acetate 80:20 v/v followed by 50:50 v/v; Yield: 15%; ^{1}H NMR (DMSO-d_6, 400 MHz) δ 9.71 (s, 1H), 8.80 (d, 1H, J = 5.6 Hz), 8.28−8.23 (m, 2H), 7.49 (d, 1H, J = 5.2 Hz), 7.32 (t, 1H, J = 8.0 Hz), 7.08 (d, 1H, J = 7.6 Hz), 7.03 (d, 1H, J = 1.6 Hz), 6.91−6.88 (m, 1H), 3.45 (s, 3H); LC/MS m/z: 357.2 (M$^+$ + 1); CHN analysis: calculated C:53.93%, H:3.39%, N:15.72%; found: C:53.82%, H:3.27%, N:15.82%.

4.4. Synthesis of the target compounds Ia-p, IIa-e, IIIa-e, IVa-e, and Va,b

The appropriate hydroxyl intermediate compound 5a,b, 7a,b, 10, or 15 (0.17 mmol) was dissolved in anhydrous DMF (1 mL), cooled to 0 °C, charged with K$_2$CO$_3$ (0.255 mmol, 36 mg) and stirred for 15 min. In reaction with sulfamoyl chloride, NaH (0.255 mmol, 10 mg) was used instead of potassium carbonate. Thenceforth, the appropriate alkyl halide or sulfamoyl chloride (0.34 mmol) dissolved in anhydrous DMF (1 mL) was added dropwise to the

reaction mixture at 0 °C and stirred at room temperature under N$_2$ $_{(g)}$ until completion. Reaction was monitored by TLC and mass spectrometry. Once reaction completion is confirmed, the mixture was quenched with ice/distilled water, extracted with ethyl acetate (3 × 5 mL), dried on rotary evaporator, and purified using normal phase column chromatography using hexane:ethyl acetate system as eluent.

4.4.1. 2-(4-(5-(2-(Methylsulfonyl)pyrimidin-4-yl)imidazo[2,1-b] thiazol-6-yl)phenoxy)-N,N-dimethylethanamine (Ia)

Purified by normal phase column chromatography, eluent dichloromethane followed by dichloromethane:methanol 85:15 v/v; Yield: 20%; ^{1}H NMR (CDCl$_3$, 400 MHz) δ 7.79 (d, 1H, J = 8.8 Hz), 7.60−7.47 (m, 4H), 7.02−6.98 (m, 3H), 3.66 (s, 3H), 3.38 (t, 2H, J = 6.4 Hz), 2.51 (t, 2H, J = 6.4 Hz), 2.32 (s, 6H); LC/MS m/z: 444.29 (M$^+$ + 1); CHN analysis: calculated C:54.16%, H:4.77%, N:15.79%; found: C:54.05%, H:4.65%, N:15.90%.

4.4.2. N-(2-(4-(5-(2-(Methylsulfonyl)pyrimidin-4-yl)imidazo[2,1-b]thiazol-6-yl)phenoxy)ethyl)-N-isopropylpropan-2-amine (Ib)

Purified by normal phase column chromatography, eluent dichloromethane followed by dichloromethane:methanol 90:10 v/v; Yield: 24%; ^{1}H NMR (CD$_3$OD, 400 MHz) δ 8.52 (d, 1H, J = 4.4 Hz), 8.16 (d, 1H, J = 5.6 Hz), 7.43−7.39 (m, 2H), 7.28 (d, 1H, J = 4.4 Hz), 7.11 (d, 1H, J = 5.6 Hz), 6.97−6.93 (m, 2H), 3.92 (t, 2H, J = 6.4 Hz), 3.21 (s, 3H), 3.05−3.00 (m, 2H), 2.95 (t, 2H, J = 6.4 Hz), 1.01 (d, 12H, J = 6.4 Hz); LC/MS m/z: 499.95 (M$^+$ + 1); CHN analysis: calculated C:57.69%, H:5.85%, N:14.02%; found: C:57.55%, H:5.81%, N:14.09%.

4.4.3. 6-(4-(2-(Pyrrolidin-1-yl)ethoxy)phenyl)-5-(2-(methylsulfonyl)pyrimidin-4-yl)imidazo[2,1-b]thiazole (Ic)

Purified by normal phase column chromatography, eluent dichloromethane followed by dichloromethane:methanol 85:15 v/v; Yield: 27%; ^{1}H NMR (CDCl$_3$, 400 MHz) δ 8.65 (d, 1H, J = 4.4 Hz), 8.25 (d, 1H, J = 5.6 Hz), 7.54−7.50 (m, 2H), 7.22−7.02 (m, 4H), 4.34 (t, 4H, J = 6.4 Hz), 3.66 (s, 3H), 3.01 (t, 4H, J = 8.0 Hz), 2.72 (t, 2H, J = 6.4 Hz), 1.01 (t, 2H, J = 6.4 Hz); LC/MS m/z: 470.03 (M$^+$ + 1); CHN analysis: calculated C:56.27%, H:4.94%, N:14.91%; found: C:56.45%, H:4.88%, N:14.80%.

4.4.4. 6-(4-(2-Morpholinoethoxy)phenyl)-5-(2-(methylsulfonyl) pyrimidin-4-yl)imidazo[2,1-b]thiazole (Id)

Purified by normal phase column chromatography, eluent ethyl acetate followed by ethyl acetate:methanol 80:20 v/v; Yield: 60%; ^{1}H NMR (CDCl$_3$, 300 MHz) δ 8.63 (d, 1H, J = 4.5 Hz), 8.19 (d, 1H, J = 5.7 Hz), 7.83−7.79 (m, 2H), 7.21 (d, 2H, J = 6.0 Hz), 7.01 (d, 2H, J = 6.0 Hz), 4.20 (t, 2H, J = 6.3 Hz), 3.77 (t, 4H, J = 5.4 Hz), 2.87 (s, 3H), 2.64 (t, 4H, J = 5.4 Hz), 1.26 (t, 2H, J = 6.3 Hz); ^{13}C NMR (CDCl$_3$, 75 MHz) δ 162.3, 159.6, 158.2, 158.0, 156.8, 154.6, 136.9, 130.5 (2C), 127.0 (2C), 122.7, 115.1, 114.4, 113.0, 66.8, 65.9, 57.6, 54.2, 54.1; LC/MS m/z: 486.35 (M$^+$ + 1); CHN analysis: calculated C:54.42%, H:4.77%, N:14.42%; found: C:54.36%, H:4.84%, N:14.33%.

4.4.5. 6-(4-(Benzyloxy)phenyl)-5-(2-(methylsulfonyl)pyrimidin-4-yl)imidazo[2,1-b]thiazole (Ie)

Purified by normal phase column chromatography, eluent hexane:ethyl acetate 80:20 v/v followed by 50:50 v/v; Yield: 20%; ^{1}H NMR (CDCl$_3$, 300 MHz) δ 8.83 (d, 1H, J = 4.4 Hz), 8.22 (d, 1H, J = 5.6 Hz), 7.87−7.74 (m, 2H), 7.48 (dd, 2H, J = 2.0, 6.8 Hz), 7.24 (d, 1H, J = 4.8 Hz), 7.11−7.03 (m, 4H), 5.16 (s, 2H), 3.23 (s, 3H); LC/MS m/z: 463.29 (M$^+$ + 1); CHN analysis: calculated C:59.72%, H:3.92%, N:12.11%; found: C:59.84%, H:3.83%, N:12.03%.

4.4.6. 5-(2-(Methylsulfonyl)pyrimidin-4-yl)-6-(4-(phenethyloxy) phenyl)imidazo[2,1-b]thiazole (If)

Purified by normal phase column chromatography, eluent hexane:ethyl acetate 90:10 v/v followed by 60:40 v/v; Yield: 32%; ^{1}H NMR (CD$_3$OD, 400 MHz) δ 8.50 (d, 1H, J = 4.4 Hz), 8.13 (d, 1H, J = 5.6 Hz), 7.39 (dd, 2H, J = 2.0, 6.8 Hz), 7.26 (d, 1H, J = 4.8 Hz), 7.27−7.22 (m, 3H), 7.19 (d, 1H, J = 1.6 Hz), 7.12 (d, 1H, J = 6.4 Hz), 7.08 (d, 1H, J = 5.6 Hz), 6.94 (dd, 2H, J = 2.0, 6.8 Hz), 4.16 (t, 2H, J = 6.8 Hz), 3.20 (s, 3H), 3.01 (t, 2H, J = 6.8 Hz); ^{13}C NMR (CD$_3$OD, 100 MHz) δ 161.5, 159.5, 158.3, 158.1, 156.9, 153.5, 153.3, 139.8, 137.0, 131.7 (2C), 130.1 (2C), 129.5 (2C), 127.5 (2C), 123.6, 116.2, 115.9, 115.4, 70.0, 36.7; LC/MS m/z: 477.34 (M$^+$ + 1); CHN analysis: calculated C:60.49%, H:4.23%, N:11.76%; found: C:60.34%, H:4.13%, N:11.89%.

4.4.7. 2-(3-(5-(2-(Methylsulfonyl)pyrimidin-4-yl)imidazo[2,1-b] thiazol-6-yl)phenoxy)-N,N-dimethylethanamine (Ig)

Purified by normal phase column chromatography, eluent ethyl acetate followed by ethyl acetate:methanol 70:30 v/v; Yield: 21%; ^{1}H NMR (CDCl$_3$, 400 MHz) δ 7.60 (d, 1H, J = 8.8 Hz), 7.32−7.28 (m, 4H), 6.98−6.94 (m, 3H), 3.62 (s, 3H), 3.22 (t, 2H, J = 6.4 Hz), 2.06 (t, 2H, J = 6.4 Hz), 1.79 (s, 6H); LC/MS m/z: 444.1 (M$^+$ + 1); CHN analysis: calculated C:54.16%, H:4.77%, N:15.79%; found: C:54.11%, H:4.62%, N:15.93%.

4.4.8. N-(2-(3-(5-(2-(Methylsulfonyl)pyrimidin-4-yl)imidazo[2,1-b]thiazol-6-yl)phenoxy)ethyl)-N-isopropylpropan-2-amine (Ih)

Purified by normal phase column chromatography, eluent ethyl acetate followed by ethyl acetate:methanol 85:15 v/v; Yield: 30%; ^{1}H NMR (CD$_3$OD, 400 MHz) δ 8.52 (d, 1H, J = 4.4 Hz), 8.18 (d, 1H, J = 5.6 Hz), 7.34−7.30 (m, 2H), 7.11 (d, 1H, J = 4.4 Hz), 7.09 (d, 1H, J = 5.6 Hz), 7.07−6.91 (m, 2H), 3.93 (t, 2H, J = 6.4 Hz), 3.15 (s, 3H), 3.12−3.10 (m, 2H), 2.90 (t, 2H, J = 6.4 Hz), 1.03 (d, 12H, J = 6.4 Hz); LC/MS m/z: 499.95 (M$^+$ + 1); CHN analysis: calculated C:57.69%, H:5.85%, N:14.02%; found: C:57.78%, H:5.90%, N:13.88%.

4.4.9. 6-(3-(2-(Pyrrolidin-1-yl)ethoxy)phenyl)-5-(2-(methylsulfonyl)pyrimidin-4-yl)imidazo[2,1-b]thiazole (Ii)

Purified by normal phase column chromatography, eluent ethyl acetate followed by ethyl acetate:methanol 85:15 v/v; Yield: 22%; ^{1}H NMR (CD$_3$OD, 400 MHz) δ 8.65 (d, 1H, J = 4.4 Hz), 8.01 (d, 1H, J = 4.8 Hz), 7.61−7.53 (m, 2H), 7.39 (d, 1H, J = 6.0 Hz), 7.23 (d, 1H, J = 6.0 Hz), 7.00−6.95 (m, 2H), 4.09 (t, 4H, J = 6.4 Hz), 3.52 (s, 3H), 2.90 (t, 4H, J = 8.0 Hz), 2.76 (t, 2H, J = 6.4 Hz), 1.06 (t, 2H, J = 6.4 Hz); LC/MS m/z: 470.1 (M$^+$ + 1); CHN analysis: calculated C:56.27%, H:4.94%, N:14.91%; found: C:56.35%, H:5.02%, N:14.83%.

4.4.10. 6-(3-(2-Morpholinoethoxy)phenyl)-5-(2-(methylsulfonyl) pyrimidin-4-yl)imidazo[2,1-b]thiazole (Ij)

Purified by normal phase column chromatography, eluent ethyl acetate followed by ethyl acetate:methanol 80:20 v/v; Yield: 45%; ^{1}H NMR (CD$_3$OD, 300 MHz) δ 8.63 (d, 1H, J = 4.5 Hz), 8.28 (d, 1H, J = 5.4 Hz), 7.47−7.40 (m, 3H), 7.22−7.11 (m, 3H), 4.20 (t, 2H, J = 5.4 Hz), 3.72 (t, 4H, J = 4.2 Hz), 2.85 (s, 3H), 2.63 (t, 4H, J = 4.2 Hz), 1.30 (t, 2H, J = 6.3 Hz); ^{13}C NMR (CD$_3$OD, 75 MHz) δ 162.0, 159.2, 157.8, 157.6, 156.4, 154.2, 136.5, 130.0 (2C), 127.0 (2C), 122.1, 121.4, 114.8, 114.3, 66.1, 65.5, 57.2, 53.7; LC/MS m/z: 486.1 (M$^+$ + 1); CHN analysis: calculated C:54.42%, H:4.77%, N:14.42%; found: C:54.30%, H:4.81%, N:14.34%.

4.4.11. 6-(3-(Benzyloxy)phenyl)-5-(2-(methylsulfonyl)pyrimidin-4-yl)imidazo[2,1-b]thiazole (Ik)

Purified by normal phase column chromatography, eluent hexane:ethyl acetate 90:10 v/v followed by 60:40 v/v; Yield: 28%; ^{1}H NMR (CDCl$_3$, 500 MHz) δ 8.87 (d, 1H, J = 4.5 Hz), 8.42 (d, 1H, J = 5.5 Hz), 7.43−7.31 (m, 7H), 7.24−7.19 (m, 2H), 7.12 (d, 1H,

$J = 8.0$ Hz), 7.60 (d, 1H, $J = 4.5$ Hz), 5.11 (s, 2H), 3.36 (s, 3H); ^{13}C NMR (CDCl$_3$, 125 MHz) δ 165.8, 159.4, 157.5, 156.9, 154.5, 153.3, 136.8, 135.6, 130.5 (2C), 128.8, 128.2, 127.6 (2C), 123.4, 121.7, 119.7, 117.8, 116.8, 115.2, 114.0, 70.2, 39.4; LC/MS *m/z*: 463.35 (M$^+$ + 1); CHN analysis: calculated C:59.72%, H:3.92%, N:12.11%; found: C:59.66%, H:3.88%, N:12.19%.

4.4.12. 6-(3-(4-Fluorobenzyloxy)phenyl)-5-(2-(methylsulfonyl) pyrimidin-4-yl)imidazo[2,1-b]thiazole (Il)

Purified by normal phase column chromatography, eluent hexane:ethyl acetate 90:10 *v/v* followed by 65:35 *v/v*; Yield: 29%; ^{1}H NMR (CD$_3$OD, 300 MHz) δ 8.46 (d, 1H, $J = 6.0$ Hz), 8.07 (d, 1H, $J = 7.2$ Hz), 7.35−7.25 (m, 4H), 7.08−6.93 (m, 6H), 4.97 (s, 2H), 3.20 (s, 3H); ^{13}C NMR (CD$_3$OD, 75 MHz) δ 160.5, 159.6, 159.2, 155.1, 136.5, 134.4, 131.4, 130.7, 130.6 (2C), 123.5, 122.9, 117.5, 116.6, 116.4, 116.1, 116.0 (2C), 115.7, 70.4, 39.6; LC/MS *m/z*: 480.8 (M$^+$ + 1); CHN analysis: calculated C:57.49%, H:3.57%, N:11.66%; found: C:57.42%, H:3.68%, N:11.56%.

4.4.13. 5-(2-(Methylsulfonyl)pyrimidin-4-yl)-6-(3-(phenethyloxy) phenyl)imidazo[2,1-b]thiazole (Im)

Purified by normal phase column chromatography, eluent hexane:ethyl acetate 90:10 *v/v* followed by 70:30 *v/v*; Yield: 25%; ^{1}H NMR (CD$_3$OD, 400 MHz) δ 8.52 (d, 1H, $J = 4.4$ Hz), 8.13 (d, 1H, $J = 5.2$ Hz), 7.33−7.28 (m, 3H), 7.19−7.15 (m, 4H), 7.10−6.98 (m, 4H), 4.13 (t, 2H, $J = 6.8$ Hz), 3.21 (s, 3H), 2.98 (t, 2H, $J = 6.8$ Hz); LC/MS *m/z*: 477.0 (M$^+$ + 1); CHN analysis: calculated C:60.49%, H:4.23%, N:11.76%; found: C:60.63%, H:4.11%, N:11.70%.

4.4.14. 6-(3-(4-Fluorophenethyloxy)phenyl)-5-(2-(methylsulfonyl) pyrimidin-4-yl)imidazo[2,1-b]thiazole (In)

Purified by normal phase column chromatography, eluent hexane:ethyl acetate 90:10 *v/v* followed by 70:30 *v/v*; Yield: 52%; ^{1}H NMR (CDCl$_3$, 400 MHz) δ 8.04 (s, 1H), 7.95 (d, 1H, $J = 8.0$ Hz), 7.74 (d, 1H, 8.0 Hz), 7.66 (t, 1H, $J = 7.5$ Hz), 7.47 (d, 1H, $J = 4.5$ Hz), 7.25−7.22 (m, 2H), 7.16 (t, 1H, $J = 8.0$ Hz), 7.05−6.98 (m, 2H), 6.93 (d, 1H, 4.5 Hz), 6.84−6.82 (m, 1H), 4.14 (t, 2H, $J = 7.0$ Hz), 3.06−3.02 (m, 5H); ^{13}C NMR (CDCl$_3$, 100 MHz) δ 161.9 (d, $J = 242.5$), 159.3, 149.9, 142.1, 134.3, 134.0 (d, $J = 3.8$ Hz), 132.1, 130.7, 130.6, 129.8, 128.7, 127.8, 127.3, 121.1, 120.6, 117.5, 115.6 (d, $J = 21.3$ Hz), 115.1, 114.4, 114.0, 68.7, 44.5, 35.1; LC/MS *m/z*: 495.0 (M$^+$ + 1); CHN analysis: calculated C:58.29%, H:3.87%, N:11.33%; found: C:58.13%, H:3.76%, N:11.45%.

4.4.15. 2-(3-(5-(2-(Methylsulfonyl)pyrimidin-4-yl)imidazo[2,1-b] thiazol-6-yl)phenoxy)-1-phenylethanone (Io)

Purified by normal phase column chromatography, eluent hexane:ethyl acetate 90:10 *v/v* followed by 55:45 *v/v*; Yield: 25%; ^{1}H NMR (CDCl$_3$, 500 MHz) δ 8.85 (d, 1H, $J = 4.5$ Hz), 8.53 (d, 1H, $J = 5.5$ Hz), 7.95−7.93 (m, 2H), 7.61 (t, 1H, $J = 7.5$ Hz), 7.49 (t, 2H, $J = 8.0$ Hz), 7.45−7.41 (m, 1H), 7.37 (d, 1H, $J = 5.5$ Hz), 7.24 (s, 1H), 7.13−7.11 (m, 2H), 7.05 (d, 1H, $J = 4.5$ Hz), 5.35 (s, 2H), 3.34 (s, 3H); ^{13}C NMR (CDCl$_3$, 125 MHz) δ 194.1, 165.8, 158.6, 157.4, 157.3, 154.4, 153.8, 135.6, 134.4, 134.2, 130.6, 129.1 (2C), 128.1 (2C), 123.4, 122.4, 119.8, 118.0, 116.9, 114.8, 114.0, 70.8, 39.4; LC/MS *m/z*: 491.32 (M$^+$ + 1); CHN analysis: calculated C:58.76%, H:3.70%, N:11.42%; found: C:58.67%, H:3.58%, N:11.55%.

4.4.16. 3-(5-(2-(Methylsulfonyl)pyrimidin-4-yl)imidazo[2,1-b] thiazol-6-yl)phenyl sulfamate (Ip)

Purified by normal phase column chromatography, eluent hexane:ethyl acetate 80:20 *v/v* followed by 50:50 *v/v*; Yield: 30%; ^{1}H NMR (Acetone-d_6, 500 MHz) δ 9.25 (d, 1H, $J = 1.5$ MHz), 8.62−8.60 (m, 1H), 8.04 (s, 2H), 7.64−7.62 (m, 1H), 7.58 (t, 1H, $J = 8.0$ MHz), 7.53−7.52 (m, 2H), 7.38−7.36 (m, 1H), 7.35 (dd, 1H, $J = 1.5$, 5.5 MHz),

3.19 (s, 3H); ^{13}C NMR (Acetone-d_6, 125 MHz) δ 158.7, 157.1, 155.0, 152.1, 150.2, 147.8, 135.8, 130.3, 127.0, 122.6, 122.5, 121.8, 120.1, 117.2, 115.1, 44.3; LC/MS *m/z*: 452.0 (M$^+$ + 1); CHN analysis: calculated C:42.56%, H:2.90%, N:15.51%; found: C:42.52%, H:2.79%, N:15.60%.

4.4.17. 6-(3-(Benzyloxy)phenyl)-5-(pyrimidin-4-yl)imidazo[2,1-b] thiazole (IIa)

Purified by normal phase column chromatography, eluent hexane:ethyl acetate 90:10 *v/v* followed by 65:35 *v/v*; Yield: 40%; ^{1}H NMR (CDCl$_3$, 500 MHz) δ 9.20 (s, 1H), 8.75 (d, 1H, $J = 4.5$ Hz), 8.41 (d, 1H, $J = 5.5$ Hz), 7.45−7.33 (m, 6H), 7.28−7.23 (m, 3H), 7.10 (d, 1H, $J = 8.0$ Hz), 6.99 (d, 1H, $J = 4.5$ Hz), 5.12 (s, 2H); ^{13}C NMR (CDCl$_3$, 125 MHz) δ 159.3, 158.7, 156.2, 156.1, 152.9, 150.9, 136.9, 136.1, 130.2, 128.7 (2C), 128.2, 127.6 (2C), 122.7, 121.9, 120.4, 116.9, 116.2, 115.2, 112.9, 70.2; LC/MS *m/z*: 385.40 (M$^+$ + 1); CHN analysis: calculated C:68.73%, H:4.19%, N:14.57%; found: C:68.88%, H:4.13%, N:14.46%.

4.4.18. 6-(3-(4-Fluorobenzyloxy)phenyl)-5-(pyrimidin-4-yl) imidazo[2,1-b]thiazole (IIb)

Purified by normal phase column chromatography, eluent hexane:ethyl acetate 95:5 *v/v* followed by 75:25 *v/v*; Yield: 55%; ^{1}H NMR (CDCl$_3$, 500 MHz) δ 9.18 (s, 1H), 8.72 (d, 1H, $J = 4.5$ Hz), 8.41 (d, 1H, $J = 5.5$ Hz), 7.40−7.35 (m, 3H), 7.26−7.21 (m, 3H), 7.07−7.04 (m, 3H), 6.97 (d, 1H, $J = 4.5$ Hz), 5.05 (s, 2H); ^{13}C NMR (CDCl$_3$, 125 MHz) δ 162.7 (d, $J = 245.0$ Hz), 159.2, 158.8, 156.2, 156.1, 153.0, 150.8, 136.1, 132.6 (d, $J = 2.5$ Hz), 130.2, 129.4 (d, $J = 7.5$ Hz), 122.7, 122.0, 120.5, 116.9, 116.2, 115.7 (d, $J = 21.3$ Hz), 115.2, 112.9, 69.6; LC/MS *m/z*: 403.36 (M$^+$ + 1); CHN analysis: calculated C:65.66%, H:3.76%, N:13.92%; found: C:65.57%, H:3.80%, N:13.86%.

4.4.19. 6-(3-(Phenethyloxy)phenyl)-5-(pyrimidin-4-yl)imidazo[2,1-b]thiazole (IIc)

Purified by normal phase column chromatography, eluent hexane:ethyl acetate 90:10 *v/v* followed by 70:30 *v/v*; Yield: 30%; ^{1}H NMR (CDCl$_3$, 500 MHz) δ 9.18 (d, 1H, $J = 1.0$ Hz), 8.73 (d, 1H, $J = 4.5$ Hz), 8.42 (d, 1H, $J = 5.5$ Hz), 7.35 (t, 1H, $J = 3.0$ Hz), 7.32−7.27 (m, 5H), 7.25−7.21 (m, 1H), 7.18−7.17 (m, 2H), 7.01−6.98 (m, 2H), 4.21 (t, 2H, $J = 7.5$ Hz), 3.11 (t, 2H, $J = 7.0$ Hz); ^{13}C NMR (CDCl$_3$, 125 MHz) δ 159.3, 158.4, 156.1, 155.7, 152.9, 150.8, 138.1, 135.7, 130.0, 129.1 (2C), 128.6 (2C), 126.5, 122.6, 121.5, 120.3, 116.8, 115.8, 114.8, 112.9, 68.8, 35.8; LC/MS *m/z*: 399.39 (M$^+$ + 1); CHN analysis: calculated C:69.32%, H:4.55%, N:14.06%; found: C:69.24%, H:4.61%, N:13.95%.

4.4.20. 6-(3-(4-Fluorophenethyloxy)phenyl)-5-(pyrimidin-4-yl) imidazo[2,1-b]thiazole (IId)

Purified by normal phase column chromatography, eluent hexane:ethyl acetate 95:5 *v/v* followed by 75:25 *v/v*; Yield: 44%; ^{1}H NMR (CDCl$_3$, 500 MHz) δ 9.19 (d, 1H, $J = 1.0$ Hz), 8.44 (d, 1H, $J = 4.5$ Hz), 8.42 (d, 1H, $J = 5.5$ Hz), 7.36 (t, 1H, $J = 8.0$ Hz), 7.28 (dd, 1H, $J = 1.0$, 5.5 Hz), 7.25−7.22 (m, 2H), 7.18−7.17 (m, 2H), 7.02−6.97 (m, 4H), 4.18 (t, 2H, $J = 7.0$ Hz), 3.06 (t, 2H, $J = 7.0$ Hz); ^{13}C NMR (CDCl$_3$, 125 MHz) δ 161.8 (d, $J = 242.5$ Hz), 159.4, 158.4, 156.3, 155.5, 153.1, 135.5, 134.0 (d, $J = 2.5$ Hz), 130.6 (d, $J = 7.5$ Hz), 130.2, 127.6, 122.8, 121.7, 120.4, 116.9, 116.1, 115.4 (d, $J = 21.3$ Hz), 114.9, 113.3, 68.9, 35.1; LC/MS *m/z*: 417.41 (M$^+$ + 1); CHN analysis: calculated C:66.33%, H:4.11%, N:13.45%; found: C:66.20%, H:4.04%, N:13.52%.

4.4.21. 2-(3-(5-(Pyrimidin-4-yl)imidazo[2,1-b]thiazol-6-yl) phenoxy)-1-phenylethanone (IIe)

Purified by normal phase column chromatography, eluent hexane:ethyl acetate 90:10 *v/v* followed by 65:35 *v/v*; Yield: 32%; ^{1}H NMR (CDCl$_3$, 500 MHz) δ 9.15 (d, 1H, $J = 1.0$ Hz), 8.70 (d, 1H, $J = 4.5$ Hz), 8.44 (d, 1H, $J = 5.5$ Hz), 7.96−7.94 (m, 2H), 7.60 (t, 1H, $J = 7.5$ Hz), 7.48 (t, 2H, $J = 8.0$ Hz), 7.38 (t, 1H, $J = 8.0$ Hz), 7.25−7.24

(m, 2H), 7.16 (s, 1H), 7.08 (dd, 1H, J = 2.0, 8.0 Hz), 6.96 (d, 1H, J = 4.5 Hz), 5.32 (s, 2H); ^{13}C NMR (CDCl$_3$, 125 MHz) δ 194.2, 158.7, 158.5, 156.4, 156.0, 152.9, 150.5, 136.1, 134.5, 134.1, 130.3, 129.0 (2C), 128.2 (2C), 122.7, 122.6, 120.5, 117.0, 116.4, 115.0, 112.9, 70.9; LC/MS m/z: 413.38 (M$^+$ + 1); CHN analysis: calculated C:66.97%, H:3.91%, N:13.58%; found: C:67.03%, H:3.86%, N:13.45%.

4.4.22. 6-(3-(Benzyloxy)phenyl)-5-phenylimidazo[2,1-b]thiazole (IIIa)

Purified by normal phase column chromatography, eluent hexane:ethyl acetate 95:5 *v/v* followed by 70:30 *v/v*; Yield: 35%; ^{1}H NMR (CDCl$_3$, 500 MHz) δ 7.46 (d, 4H, J = 3.5 Hz), 7.43–7.39 (m, 1H), 7.36–7.32 (m, 7H), 7.19–7.16 (m, 2H), 6.87 (d, 1H, J = 7.5 Hz), 6.80 (d, 1H, J = 4.5 Hz), 4.96 (s, 2H); ^{13}C NMR (CDCl$_3$, 125 MHz) δ 158.9, 149.0, 143.2, 137.2, 135.8, 130.5, 129.4, 129.3 (2C), 128.6 (2C), 127.9 (2C), 127.6 (2C), 123.1, 120.4, 117.6, 114.8, 113.2, 112.7, 69.9; LC/MS m/z: 383.39 (M$^+$ + 1); CHN analysis: calculated C:75.37%, H:4.74%, N:7.32%; found: C:75.32%, H:4.69%, N:7.40%.

4.4.23. 6-(3-(4-Fluorobenzyloxy)phenyl)-5-phenylimidazo[2,1-b]thiazole (IIIb)

Purified by normal phase column chromatography, eluent hexane:ethyl acetate 95:5 *v/v* followed by 75:25 *v/v*; Yield: 40%; ^{1}H NMR (CDCl$_3$, 500 MHz) δ 7.47–7.45 (m, 4H), 7.43–7.42 (m, 1H), 7.36 (d, 1H, J = 4.5 Hz), 7.33–7.29 (m, 3H), 7.18–7.15 (m, 2H), 7.05–7.01 (m, 2H), 6.85–6.83 (m, 1H), 6.81 (d, 1H, J = 5.0 Hz), 4.92 (s, 2H); ^{13}C NMR (CDCl$_3$, 125 MHz) δ 162.5 (d, J = 244.4 Hz), 158.8, 149.0, 143.2, 135.9, 133.0 (d, J = 3.8 Hz), 130.6, 129.5, 129.4, 129.4, 129.3, 128.6, 123.1, 120.5, 117.6, 115.5 (d, J = 21.3 Hz), 114.8, 113.2, 112.7, 69.3; LC/MS m/z: 401.35 (M$^+$ + 1); CHN analysis: calculated C:71.98%, H:4.28%, N:7.00%; found: C:71.89%, H:4.13%, N:7.14%.

4.4.24. 6-(3-(Phenethyloxy)phenyl)-5-phenylimidazo[2,1-b]thiazole (IIIc)

Purified by normal phase column chromatography, eluent hexane:ethyl acetate 95:5 *v/v* followed by 75:25 *v/v*; Yield: 53%; ^{1}H NMR (CDCl$_3$, 500 MHz) δ 7.46–7.42 (m, 4H), 7.40–7.35 (m, 2H), 7.32–7.29 (m, 2H), 7.23–7.21 (m, 4H), 7.17–7.13 (m, 2H), 6.82 (d, 1H, J = 4.5 Hz), 6.80–6.76 (m, 1H), 4.07 (t, 2H, J = 7.5 Hz), 3.02 (t, 2H, J = 7.5 Hz); ^{13}C NMR (CDCl$_3$, 125 MHz) δ 158.9, 148.9, 143.1, 138.5, 135.6, 130.5, 129.5, 129.4, 129.4, 129.1, 128.6, 128.5, 126.5, 123.1, 120.2, 117.6, 114.6, 113.1, 112.8, 68.6, 35.8; LC/MS m/z: 397.44 (M$^+$ + 1); CHN analysis: calculated C:75.73%, H:5.08%, N:7.07%; found: C:75.62%, H:5.05%, N:7.11%.

4.4.25. 6-(3-(4-Fluorophenethyloxy)phenyl)-5-phenylimidazo[2,1-b]thiazole (IIId)

Purified by normal phase column chromatography, eluent hexane:ethyl acetate 95:5 *v/v* followed by 75:25 *v/v*; Yield: 28%; ^{1}H NMR (CDCl$_3$, 500 MHz) δ 7.48–7.43 (m, 4H), 7.41–7.35 (m, 2H), 7.22–7.13 (m, 5H), 7.00–6.96 (m, 2H), 6.84 (d, 1H, J = 4.5 Hz), 6.79–6.76 (m, 1H), 4.06 (t, 2H, J = 7.0 Hz), 2.99 (t, 2H, J = 7.0 Hz); ^{13}C NMR (CDCl$_3$, 125 MHz) δ 161.8 (d, J = 242.7 Hz), 158.9, 148.9, 134.2 (d, J = 3.4 Hz), 130.6 (d, J = 7.6 Hz), 130.34, 129.5, 129.5, 129.4, 128.7, 128.6, 127.6, 123.1, 120.2, 117.7, 115.3 (d, J = 20.9 Hz), 114.7, 113.1, 113.0, 68.6, 35.0; LC/MS m/z: 415.27 (M$^+$ + 1); CHN analysis: calculated C:72.44%, H:4.62%, N:6.76%; found: C:72.50%, H:4.55%, N:6.68%.

4.4.26. 2-(3-(5-Phenylimidazo[2,1-b]thiazol-6-yl)phenoxy)-1-phenylethanone (IIIe)

Purified by normal phase column chromatography, eluent hexane:ethyl acetate 95:5 *v/v* followed by 75:25 *v/v*; Yield: 55%; ^{1}H NMR (CDCl$_3$, 500 MHz) δ 7.93 (d, 2H, J = 7.5 Hz), 7.61 (t, 1H, J = 7.5 Hz), 7.49 (t, 2H, J = 7.5 Hz), 7.43–7.40 (m, 4H), 7.36–7.35 (m,

2H), 7.25–7.17 (m, 3H), 6.90–6.89 (m, 1H), 6.83 (d, 1H, J = 3.5 Hz), 5.16 (s, 2H); ^{13}C NMR (CDCl$_3$, 125 MHz) δ 194.3, 158.2, 148.9, 142.7, 135.6, 134.7, 133.9, 130.3, 129.7, 129.5, 129.4, 128.9, 128.7, 128.3, 123.2, 121.0, 117.6, 115.2, 113.1, 112.9, 70.8; LC/MS m/z: 411.36 (M$^+$ + 1); CHN analysis: calculated C:73.15%, H:4.42%, N:6.82%; found: C:73.04%, H:4.37%, N:6.91%.

4.4.27. 6-(3-(Benzyloxy)phenyl)-5-(3-(methylsulfonyl)phenyl)imidazo[2,1-b]thiazole (IVa)

Purified by normal phase column chromatography, eluent hexane:ethyl acetate 90:10 *v/v* followed by 55:45 *v/v*; Yield: 25%; ^{1}H NMR (CDCl$_3$, 500 MHz) δ 8.04 (t, 1H, J = 1.5 Hz), 7.96–7.94 (m, 1H), 7.74 (dt, 1H, J = 1.5, 8.0 Hz), 7.65 (t, 1H, J = 3.0 Hz), 7.46 (d, 1H, J = 4.5 Hz), 7.39–7.35 (m, 4H), 7.33–7.31 (m, 1H), 7.21 (t, 1H, J = 8.0 Hz), 7.12–7.10 (m, 1H), 6.95 (d, 1H, J = 4.5 Hz), 6.92–6.90 (m, 1H), 5.03 (s, 2H), 3.03 (s, 3H); ^{13}C NMR (CDCl$_3$, 125 MHz) δ 159.2, 150.0, 142.0, 137.0, 134.1, 132.0, 130.5, 129.8, 128.7, 128.1 (2C), 127.7 (2C), 127.0 (2C), 121.0, 120.7, 117.4, 115.0, 114.2, 114.0, 70.2, 44.5; LC/MS m/z: 461.33 (M$^+$ + 1); CHN analysis: calculated C:65.20%, H:4.38%, N:6.08%; found: C:65.37%, H:4.22%, N:6.04%.

4.4.28. 6-(3-(4-Fluorobenzyloxy)phenyl)-5-(3-(methylsulfonyl)phenyl)imidazo[2,1-b]thiazole (IVb)

Purified by normal phase column chromatography, eluent hexane:ethyl acetate 90:10 *v/v* followed by 55:45 *v/v*; Yield: 40%; ^{1}H NMR (CDCl$_3$, 500 MHz) δ 8.04–8.04 (m, 1H), 7.96–7.94 (m, 1H), 7.74–7.73 (m, 1H), 7.65 (t, 1H, J = 7.5 Hz), 7.45 (d, 1H, J = 4.5 Hz), 7.38–7.35 (m, 2H), 7.28–7.28 (m, 1H), 7.19 (t, 1H, 8.0 Hz) 7.10–7.04 (m, 3H), 6.93 (d, 1H, J = 4.5 Hz), 6.90–6.88 (m, 1H), 4.99 (s, 2H), 3.04 (s, 3H); ^{13}C NMR (CDCl$_3$, 125 MHz) δ 162.6 (d, J = 245.0 Hz), 150.1, 142.0, 134.0, 132.8 (d, J = 3.8 Hz), 132.1, 130.5, 129.7, 129.5 (d, J = 8.8 Hz), 127.7, 126.9, 121.0, 120.8, 117.3, 115.6 (d, J = 21.8 Hz), 115.0, 114.1, 113.8, 69.5, 44.5; LC/MS m/z: 479.35 (M$^+$ + 1); CHN analysis: calculated C:62.74%, H:4.00%, N:5.85%; found: C:62.69%, H:3.92%, N:5.92%.

4.4.29. 5-(3-(Methylsulfonyl)phenyl)-6-(3-(phenethyloxy)phenyl)imidazo[2,1-b]thiazole (IVc)

Purified by normal phase column chromatography, eluent hexane:ethyl acetate 90:10 *v/v* followed by 55:45 *v/v*; Yield: 34%; ^{1}H NMR (CDCl$_3$, 500 MHz) δ 8.01 (s, 1H), 7.92 (d, 1H, J = 8.0 Hz), 7.72 (d, 1H, J = 7.5 Hz), 7.63 (t, 1H, J = 8.0 Hz), 7.43 (d, 1H, J = 4.5 Hz), 7.32–7.29 (m, 2H), 7.25–7.23 (m, 3H), 7.19–7.15 (m, 2H), 7.06 (d, 1H, J = 7.5 Hz), 6.90 (d, 1H, J = 4.5 Hz), 6.82 (dd, 1H, J = 2.0, 8.0 Hz), 4.12 (t, 2H, J = 7.0 Hz), 3.05 (t, 2H, J = 7.0 Hz), 2.96 (s, 3H); ^{13}C NMR (CDCl$_3$, 125 MHz) δ 159.1, 150.2, 144.9, 141.9, 138.4, 135.3, 134.1, 132.3, 130.4, 129.6, 129.1, 128.6, 127.7 (2C), 126.8 (2C), 126.6, 120.9, 120.5, 117.3, 114.6, 113.9, 113.6, 68.8, 44.4, 35.9; LC/MS m/z: 475.38 (M$^+$ + 1); CHN analysis: calculated C:65.80%, H:4.67%, N:5.90%; found: C:65.77%, H:4.60%, N:5.97%.

4.4.30. 6-(3-(4-Fluorophenethyloxy)phenyl)-5-(3-(methylsulfonyl)phenyl)imidazo[2,1-b]thiazole (IVd)

Purified by normal phase column chromatography, eluent hexane:ethyl acetate 90:10 *v/v* followed by 55:45 *v/v*; Yield: 30%; ^{1}H NMR (CDCl$_3$, 500 MHz) δ 8.02 (s, 1H), 7.94 (d,1H, J = 8.0 Hz), 7.72 (d, 1H, 8.0 Hz), 7.64 (t, 1H, J = 7.5 Hz), 7.44 (d, 1H, J = 4.5 Hz), 7.22–7.20 (m, 3H), 7.15 (t, 1H, J = 8.0 Hz), 7.03–6.97 (m, 3H), 6.92 (d, 1H, 4.5 Hz), 6.82–6.80 (m, 1H), 4.12 (t, 2H, J = 7.0 Hz), 3.04–3.00 (m, 5H); ^{13}C NMR (CDCl$_3$, 125 MHz) δ 161.8 (d, J = 242.5 Hz), 159.2, 149.9, 142.0, 134.1, 134.1 (d, J = 3.8 Hz), 131.9, 130.6, 130.5, 129.7, 128.7, 128.2, 127.8 (2C), 127.7 (2C), 127.1, 121.0, 120.5, 117.4, 115.4 (d, J = 21.3 Hz), 115.0, 114.2, 113.8, 68.7, 44.4, 35.1; LC/MS m/z: 493.34 (M$^+$ + 1); CHN analysis: calculated C:63.40%, H:4.30%, N:5.69%; found: C:63.30%, H:4.24%, N:5.77%.

4.4.31. 2-(3-(5-(3-(Methylsulfonyl)phenyl)imidazo[2,1-b]thiazol-6-yl)phenoxy)-1-phenylethanone (IVe)

Purified by normal phase column chromatography, eluent hexane:ethyl acetate 90:10 *v/v* followed by 55:45 *v/v*; Yield: 40%; ^{1}H NMR (DMSO-d_6, 500 MHz) δ 8.02 (s, 1H), 7.97−7.95 (m, 1H), 7.92 (d, 1H, J = 4.5 Hz), 7.85 (d, 1H, J = 8.0 Hz), 7.75 (d, 1H, J = 8.0 Hz), 7.70 (d, 1H, J = 7.5 Hz), 7.62−7.61 (m, 1H), 7.58 (t, 2H, J = 7.5 Hz), 7.50 (d, 1H, J = 4.5 Hz), 7.33 (d, 1H, J = 6.5 Hz), 7.28 (t, 1H, J = 8.0 Hz), 7.08−7.07 (m, 2H), 6.96−6.94 (m, 1H), 5.51 (s, 2H), 3.24 (s, 3H); ^{13}C NMR (DMSO-d_6, 125 MHz) δ 194.3, 158.1, 148.5, 148.2, 141.8, 134.3, 134.2, 133.9, 130.6, 129.8, 128.9, 128.5, 127.8, 127.7 (2C), 127.6, 127.2 (2C), 125.5, 120.1, 119.1, 115.9, 114.6, 113.5, 70.1, 43.4; LC/MS *m/z*: 489.3 (M$^+$ + 1); CHN analysis: calculated C:63.92%, H:4.13%, N:5.73%; found: C:63.83%, H:4.02%, N:5.88%.

4.4.32. 6-(3-(Benzyloxy)phenyl)-5-(2-(methylsulfonyl)pyrimidin-4-yl)imidazo[2,1-b]oxazole (Va)

Purified by normal phase column chromatography, eluent hexane:ethyl acetate 80:20 *v/v* followed by 30:70 *v/v*; Yield: 15%; ^{1}H NMR (CD$_3$CN, 500 MHz) δ 8.54 (d, 1H, J = 2.5 Hz), 8.36 (d, 1H, J = 3.0 Hz), 7.69−7.60 (m, 5H), 7.39−7.28 (m, 5H), 7.13 (d, 1H, J = 9.0 Hz), 5.01 (s, 2H), 3.28 (s, 3H); ^{13}C NMR (CD$_3$CN, 125 MHz) δ 163.7, 155.4, 148.8, 143.3, 140.3, 138.3, 137.5, 132.3, 132.0, 130.5, 129.7, 128.9, 128.8 (2C), 128.2 (2C), 124.6, 122.5, 122.0, 119.3, 116.1, 68.7, 39.6; LC/MS *m/z*: 447.34 (M$^+$ + 1).

4.4.33. 6-(3-(4-Fluorobenzyloxy)phenyl)-5-(2-(methylsulfonyl) pyrimidin-4-yl)imidazo[2,1-b]oxazole (Vb)

Purified by normal phase column chromatography, eluent hexane:ethyl acetate 80:20 *v/v* followed by 40:60 *v/v*; Yield: 20%; ^{1}H NMR (DMSO-d_6, 500 MHz) δ 8.21 (d, 1H, J = 2.0 Hz), 7.67 (d, 1H, J = 1.5 Hz), 7.60 (d, 1H, J = 7.0 Hz), 7.46−7.44 (m, 2H), 7.40−7.36 (m, 3H), 7.21 (d, 1H, J = 2.0 Hz)), 7.14−7.06 (m, 2H), 6.24 (d, 1H, J = 7.0 Hz), 4.98 (s, 2H), 3.55 (s, 3H); ^{13}C NMR (DMSO-d_6, 125 MHz) δ 161.9, 158.2, 155.8, 155.2, 149.2, 148.6, 140.1, 135.6, 133.2, 132.8 (d, J = 2.8 Hz), 130.2 (d, J = 8.1 Hz), 129.9 (d, J = 8.3 Hz), 122.1, 116.1, 115.9, 115.6, 115.4, 115.2, 115.0, 69.8, 39.2; LC/MS *m/z*: 465.3 (M$^+$ + 1).

4.5. Antiproliferative screening

It was conducted at the National Cancer Institute (NCI, USA) using the standard protocol published on their official website [https://dtp.cancer.gov/discovery_development/nci-60/methodology.htm].

4.6. Kinase profiling

The kinase was incubated with 8 mM MOPS pH 7.0, 0.2 mM EDTA, 2.5 mM MnCl2, 0.1 mg/mL poly(Glu, Tyr) 4:1, 10 mM magnesium acetate and [γ^{33}P]-ATP (specific activity ~500 cpm/pmol, 1 μM concentration). The reaction was initiated by the addition of the Mg/ATP mix. After incubation for 40 min at room temperature, the reaction was stopped by addition of phosphoric acid to a concentration of 0.5%. 10 μL of the reaction was then spotted onto a Filtermat A and washed four times for 4 min in 0.425% phosphoric acid and once in methanol prior to drying and scintillation counting [22].

4.7. In-cell ErbB4 kinase assay

In the cellular ErbB4 phosphorylation assay the human breast cancer cell line T-47D is used, which endogenously expresses a high level of ErbB4. Stimulation of these cells with human neuregulin 1 (NRG1) results in receptor tyrosine autophosphorylation. T-47D cells were plated in RPMI supplemented with 10% FCS in multiwell cell culture plates. Next day, medium was exchanged for serum-free medium and compounds were added (90 min at 37 °C). Cells treated with 1,0E-05 M lapatinib were used as low control. For stimulation, cells were treated with 100 ng/mL neuregulin 1 for 5 min at room temperature. After cell lysis quantification of receptor autophosphorylation was assessed in 96-well plates *via* sandwich-ELISA using a kinase specific capture antibody and an anti-phosphotyrosine detection antibody [22].

4.8. hERG ion channel assay

The assay depends on the competition of fluorescently labeled tracer binding to the membrane preparation containing hERG. A buffer composed of 25 mM Hepes, pH 7.5, 15 mM KCl, 1 mM MgCl$_2$, 0.05% PF-127, and 1% DMSO was used. Solutions of compounds Ik, IIa, and the reference compound E−4031 in DMSO were added in the test concentration into the membrane mixture (1X Predictor™ hERG Membrane) utilizing Acoustic Technology. The tracer (1 nM Predictor™ hERG Tracer Red) was added and gently mixed in the dark. The fluorescence was measured at 531 nm after 3 h incubation in the dark at room temperature and the membrane potential was measured. The background was established by the average FP signal in the presence of E−4031 (30 μM). The dose-response curves were prepared using GraphPad Prism (version 6.01) software [36].

4.9. Testing against CYP 2D6 and 3A4

The assay is based on the fluorescence read out using Vivid® fluorescence substrates against CYP BACULOSOMES® from ThermoFisher Scientific. CYP 26 or 3A4 was prepared with regeneration system (333 mM glucose-6-phosphate and 30 U/mL glucose-6-phosphate dehydrogenase in 100 mM potassium phosphate, pH 8.0) and substrate (10 μM Vivid® EOMCC substrate in case of CYP 2D6 or 10 μM Vivid® BOMCC substrate in case of CYP 3A4) with NADP$^+$ (10 mM) in freshly prepared reaction buffer (100 mM potassium phosphate buffer (pH 8.0), and 1% DMSO). The enzyme solution was delivered into the reaction wells. Compound Ik, IIa, or ketoconazole solution in 100% DMSO was delivered into the enzyme solution by Acoustic technology (Echo550; nanoliter range) and incubated for 20 min at room temperature. The substrate solution was then delivered into the reaction well to initiate the reaction. The enzyme activities were monitored as a time-course measurement of the increase in fluorescence signal from fluorescence substrate for 100 min at room temperature in EnVision. Data analysis was carried out by taking slope (signal/min) of linear portion of time course measurement, and %enzyme activity was calculated relative to DMSO control (https://assets.thermofisher.com/TFS-Assets/LSG/manuals/Vivid_CYP450_Screening_Kits_man.pdf).

4.10. Computational studies

The X-ray crystal structure of ErbB4 (HER4) kinase complexed with thienopyrimidine inhibitor was retrieved from the RSCB protein data bank (http://www.rcsb.org/under the entry code (PDB ID: 2R4B, Resolution: 2.4 Å). Molecular docking procedure was carried-on employing the program Autodock Vina® [37]. The complexed inhibitor was extracted from the initial X-ray structure followed by removal of water molecules. Polar hydrogens and Gastieger charges were added and the corresponding charge files were generated using the MGL Tools. The compounds under study were drawn using ChemDraw® Ultra v8.0 (Cambridge Soft Corporation, USA) and were optimised for energy and geometry using

MMFF94 force field. Furthermore, a grid box was established to cover the enzyme active site with a spacing of 1.0 Å between the grid points. The box was centered toward the coordinates of ($-15.61 \times 16.91 \times$ -1.81). The exhaustiveness and the number of poses were set to 12 and 10, respectively. The 3D-best docked poses were visualized using PyMOL molecular viewer (Schrödinger Inc., New York, NY, USA). Later, the best docked-pose of compound **Ik** complexed with ErbB4 kinase was subjected to molecular dynamic simulation employing the Desmond® v3.8 software [38] embedded within Maestro® v9.8 graphical interface [39]. All-atoms molecular dynamic simulation protocol was adapted as mentioned in Ref. [40], and the results were visualized *via* the Desmond® simulation interaction diagram panel.

Declaration of competing interest

None.

Acknowledgments

Appendix A. Supplementary data

Supplementary data to this article can be found online at https://doi.org/10.1016/j.ejmech.2021.113674.

References

[1] J. Ferlay, M. Laversanne, M. Ervik, F. Lam, M. Colombet, L. Mery, M. Piñeros, A. Znaor, I. Soerjomataram, F. Bray, Global cancer observatory, in: Cancer Tomorrow, International Agency for Research on Cancer, Lyon, France, 2020.

[2] T. Hunter, J.A. Cooper, Protein-tyrosine kinases, Annu. Rev. Biochem. 54 (1985) 897−930.

[3] B.J. Druker, STI571 (Gleevec™) as a paradigm for cancer therapy, Trends Mol. Med. 8 (2002) S14−S18.

[4] D.F. Stern, ERBB3/HER3 and ERBB2/HER2 duet in mammary development and breast cancer, J. Mammary Gland Biol. Neoplasia 13 (2008) 215.

[5] E.M. Bublil, Y. Yarden, The EGF receptor family: spearheading a merger of signaling and therapeutics, Curr. Opin. Cell Biol. 19 (2007) 124−134.

[6] Y. Zhu, L.L. Sullivan, S.S. Nair, C.C. Williams, A.K. Pandey, L. Marrero, R.K. Vadlamudi, F.E. Jones, Coregulation of estrogen receptor by ERBB4/HER4 establishes a growth-promoting autocrine signal in breast tumor cells, Canc. Res. 66 (2006) 7991.

[7] J. Edwards, P. Traynor, A.F. Munro, C.F. Pirret, B. Dunne, J.M.S. Bartlett, The role of HER1-HER4 and EGFRvIII in hormone-refractory prostate cancer, Clin. Canc. Res. 12 (2006) 123.

[8] C.S. Williams, J.K. Bernard, M. Demory Beckler, D. Almohazey, M.K. Washington, J.J. Smith, M.R. Frey, ERBB4 is over-expressed in human colon cancer and enhances cellular transformation, Carcinogenesis 36 (2015) 710−718.

[9] L.M.R. Gilmour, K.G. Macleod, A. McCaig, W.J. Gullick, J.F. Smyth, S.P. Langdon, Expression of erbB-4/HER-4 growth factor receptor isoforms in ovarian cancer, Canc. Res. 61 (2001) 2169.

[10] V.F.M. Segers, L. Dugaucquier, E. Feyen, H. Shakeri, G.W. De Keulenaer, The role of ErbB4 in cancer, Cell. Oncol. 43 (2020) 335−352.

[11] H. Xie, L. Lin, L. Tong, Y. Jiang, M. Zheng, Z. Chen, X. Jiang, X. Zhang, X. Ren, W. Qu, Y. Yang, H. Wan, Y. Chen, J. Zuo, H. Jiang, M. Geng, J. Ding, AST1306, A novel irreversible inhibitor of the epidermal growth factor receptor 1 and 2, exhibits antitumor activity both in vitro and in vivo, PloS One 6 (2011), e21487.

[12] T.M. Kim, K.-W. Lee, D.-Y. Oh, J.-S. Lee, S.-A. Im, D.-W. Kim, S.-W. Han, Y.J. Kim, T.-Y. Kim, J.H. Kim, H. Han, W.H. Kim, Y.-J. Bang, Phase 1 studies of poziotinib, an irreversible pan-HER tyrosine kinase inhibitor in patients with advanced solid tumors, Cancer Res Treat 50 (2018) 835−842.

[13] D. Lavacchi, F. Mazzoni, G. Giaccone, Clinical evaluation of dacomitinib for the treatment of metastatic non-small cell lung cancer (NSCLC): current perspectives, Drug Des. Dev. Ther. 13 (2019) 3187−3198.

[14] A. Joan, G. Pere, Small molecules with EGFR-TK inhibitor activity, Curr. Drug Targets 6 (2005) 259−274.

[15] E.R. Wood, A.T. Truesdale, O.B. McDonald, D. Yuan, A. Hassell, S.H. Dickerson, B. Ellis, C. Pennisi, E. Horne, K. Lackey, K.J. Alligood, D.W. Rusnak, T.M. Gilmer, L. Shewchuk, A unique structure for epidermal growth factor receptor bound to GW572016 (lapatinib), Canc. Res. 64 (2004) 6652.

[16] F. Rauf, F. Festa, J.G. Park, M. Magee, S. Eaton, C. Rinaldi, C.M. Betanzos, L. Gonzalez-Malerva, J. LaBaer, Ibrutinib inhibition of ERBB4 reduces cell growth in a WNT5A-dependent manner, Oncogene 37 (2018) 2237−2250.

[17] H. Modjtahedi, B.C. Cho, M.C. Michel, F. Solca, A comprehensive review of the preclinical efficacy profile of the ErbB family blocker afatinib in cancer, N. Schmied. Arch. Pharmacol. 387 (2014) 505−521.

[18] S.R. Tiwari, P. Mishra, J. Abraham, Neratinib, A novel HER2-targeted tyrosine kinase inhibitor, Clin. Breast Canc. 16 (2016) 344−348.

[19] Q. Chen, D. Ouyang, M. Anwar, N. Xie, S. Wang, P. Fan, L. Qian, G. Chen, E. Zhou, L. Guo, X. Gu, B. Ding, X. Yang, L. Liu, C. Deng, Z. Xiao, J. Li, Y. Wang, S. Zeng, J. Hu, W. Zhou, B. Qiu, Z. Wang, J. Weng, M. Liu, Y. Li, T. Tang, J. Wang, H. Zhang, B. Dai, W. Tang, T. Wu, M. Xiao, X. Li, H. Liu, L. Li, W. Yi, Q. Ouyang, Effectiveness and safety of pyrotinib, and association of biomarker with progression-free survival in patients with HER2-positive metastatic breast cancer: a real-world, multicentre analysis, Front Oncol 10 (2020), 811-811.

[20] J.B. Smaill, G.W. Rewcastle, J.A. Loo, K.D. Greis, O.H. Chan, E.L. Reyner, E. Lipka, H.D.H. Showalter, P.W. Vincent, W.L. Elliott, W.A. Denny, Tyrosine kinase inhibitors. 17. Irreversible inhibitors of the epidermal growth factor Receptor: 4-(phenylamino)quinazoline- and 4-(Phenylamino)pyrido[3,2-d]pyrimidine-6-acrylamides bearing additional solubilizing functions, J. Med. Chem. 43 (2000) 1380−1397.

[21] M. Ashwell, M. Tandon, J.-M. Lapierre, Synthesis of imidazooxazole and imidazothiazole inhibitors of p38 map kinase, in: WIPO IP Portal, 2006.

[22] H.S. Anbar, M.I. El-Gamal, H. Tarazi, B.S. Lee, H.R. Jeon, D. Kwon, C.-H. Oh, Imidazothiazole-based potent inhibitors of V600E-B-RAF kinase with promising anti-melanoma activity: biological and computational studies, J. Enzym. Inhib. Med. Chem. 35 (2020) 1712−1726.

[23] J.-H. Park, M.I. El-Gamal, Y.S. Lee, C.-H. Oh, New imidazo[2,1-b]thiazole derivatives: synthesis, in vitro anticancer evaluation, and in silico studies, Eur. J. Med. Chem. 46 (2011) 5769−5777.

[24] M.G. El-Din, C.H. Seok, Y.K. Ho, H.D. Keun, O.C. Hyun, M. Abdel-Maksoud, M.I. El-Gamal, Imidazooxazole derivative having antitumor effect, and pharmaceutical composition including same, in: WIPO IP Portal, 2017.

[25] M.S. Abdel-Maksoud, M.-R. Kim, M.I. El-Gamal, M.M. Gamal El-Din, J. Tae, H.S. Choi, K.-T. Lee, K.H. Yoo, C.-H. Oh, Design, synthesis, in vitro antiproliferative evaluation, and kinase inhibitory effects of a new series of imidazo[2,1-b]thiazole derivatives, Eur. J. Med. Chem. 95 (2015) 453−463.

[26] R.M. Sbenati, M.H. Semreen, A.M. Semreen, M.K. Shehata, F.M. Alsaghir, M.I. El-Gamal, Evaluation of imidazo[2,1-b]thiazole-based anticancer agents in one decade (2011-2020): current status and future prospects", Bioorg. Med. Chem. 29 (2021) 115897.

[27] M.S. Abdel-Maksoud, M.I. El-Gamal, B.S. Lee, M.M. Gamal El-Din, H.R. Jeon, D. Kwon, U.M. Ammar, K.I. Mersal, E.M.H. Ali, K.-T. Lee, K.H. Yoo, D.K. Han, J.K. Lee, G. Kim, H.S. Choi, Y.J. Kwon, K.H. Lee, Chang-Hyun Oh, Discovery of new imidazo[2,1-b]thiazole derivatives as potent pan-RAF inhibitors with promising in vitro and in vivo anti-melanoma activity, J. Med. Chem. 64 (2021) 6877−6901.

[28] V.B. Wali, J.W. Haskins, M. Gilmore-Hebert, J.T. Platt, Z. Liu, D.F. Stern, Convergent and divergent cellular responses by ErbB4 isoforms in mammary epithelial cells, Mol. Canc. Res. 12 (2014) 1140.

[29] W. Haverkamp, G. Breithardt, A.J. Camm, M.J. Janse, M.R. Rosen, C. Antzelevitch, D. Escande, M. Franz, M. Malik, A. Moss, R. Shah, The potential for QT prolongation and proarrhythmia by non-antiarrhythmic drugs: clinical and regulatory implications. Report on a Policy Conference of the European Society of Cardiology, Eur. Heart J. 21 (2000) 1216−1231.

[30] L. Kiss, P.B. Bennett, V.N. Uebele, K.S. Koblan, S.A. Kane, B. Neagle, K. Schroeder, High throughput ion-channel pharmacology: planar-array-based voltage clamp, Assay Drug Dev. Technol. 1 (2003) 127−135.

[31] K. Schroeder, B. Neagle, D.J. Trezise, J. Worley, H.T. IonWorks™, A new high-throughput electrophysiology measurement platform, J. Biomol. Screen 8 (2003) 50−64.

[32] D.J. Greenblatt, Y. Zhao, K. Venkatakrishnan, S.X. Duan, J.S. Harmatz, S.J. Parent, M.H. Court, L.L. von Moltke, Mechanism of cytochrome P450-3A inhibition by ketoconazole, J. Pharm. Pharmacol. 63 (2011) 214−221.

[33] U. Bren, C. Oostenbrink, Cytochrome P450 3A4 inhibition by ketoconazole: tackling the problem of ligand cooperativity using molecular dynamics simulations and free-energy calculations, J. Chem. Inf. Model. 52 (2012) 1573−1582.

[34] X. Zhang, J. Gureasko, K. Shen, P.A. Cole, J. Kuriyan, An allosteric mechanism for activation of the kinase domain of epidermal growth factor receptor, Cell 125 (2006) 1137−1149.

[35] N. Jura, X. Zhang, Nicholas F. Endres, Markus A. Seeliger, T. Schindler, J. Kuriyan, Catalytic control in the EGF receptor and its connection to general kinase regulatory mechanisms, Mol. Cell 42 (2011) 9−22.

[36] R.M. Sbenati, S.-O. Zaraei, M.I. El-Gamal, H.S. Anbar, H. Tarazi, M.M. Zoghbor, N.A. Mohamood, M.M. Khakpour, D.M. Zaher, H.A. Omar, N.N. Alach, M.K. Shehata, R. El-Gamal, Design, synthesis, biological evaluation, and modeling studies of novel conformationally-restricted analogues of sorafenib as selective kinase-inhibitory antiproliferative agents against hepatocellular carcinoma cells, Eur. J. Med. Chem. 210 (2021) 113081.

[37] O. Trott, A.J. Olson, AutoDock Vina, Improving the speed and accuracy of docking with a new scoring function, efficient optimization, and

multithreading, J. Comput. Chem. 31 (2010) 455–461.

[38] K.J. Bowers, E. Chow, H. Xu, R.O. Dror, M.P. Eastwood, B.A. Gregersen, J.L. Klepeis, I. Kolossvary, M.A. Moraes, F.D. Sacerdoti, J.K. Salmon, Y. Shan, D.E. Shaw, Scalable algorithms for molecular dynamics simulations on commodity clusters, in: Proceedings of the 2006 ACM/IEEE Conference on Supercomputing, Association for Computing Machinery, Tampa, Florida, 2006,

84–es.

[39] Schrödinger Release 2014-2: Maestro, Version 9.8, Schrödinger, LLC, New York, NY, 2014.

[40] H. Tarazi, M.I. El-Gamal, C.-H. Oh, Discovery of highly potent V600E-B-RAF kinase inhibitors: molecular modeling study, Bioorg. Med. Chem. 27 (2019) 655–663.